

Solar Powered Lighting for Overhead Highway Signs*

**(Prepared in Cooperation with the US Department of Transportation, Federal Highway Administration, MBTC and AHTD under Grant Number MBTC 2096)*

FINAL REPORT

PI: Hiram C. Patangia, Ph.D., P.E.
University of Arkansas @ Little Rock
2801 S. University, ETAS 227
Little Rock, AR 72204
501.569.8202(v)
501.569.8206(f)
hccpatangia@ualr.edu

ACKNOWLEDGEMENT

The author wishes to acknowledge the financial support of Mack-Blackwell Rural Transportation Center and Arkansas Highway & Transportation Department for the project under grant MBTC-2096. We would like to extend our gratitude to Mike Sobba who volunteered his time, equipment, and expertise in fabricating and installing the solar panel mounting structures. The technical support of HK Idea-Tech. toward the project is greatly appreciated. Thanks are also due to my students especially Dennis Gregory for his commendable technical support throughout the project.

Disclaimer Statement

The contents of this report reflect the views of the author who is responsible for the facts and the accuracy of the data presented herein. The document is disseminated under the sponsorship of Department of Transportation, University Transportation Centers Program, and Arkansas Highway and Transportation Department, in the interest of information exchange. The U.S. Government assumes no liability for the contents or use thereof. This report does not constitute a standard, specification, or regulation.

Project Abstract

The purpose of the research is to design and develop a low cost solar powered lighting system for overhead highway signs with a view to improving night visibility especially under poor driving conditions, and enhance highway safety. Two lighting systems have been researched, developed and tested: one system employs LED technology and the other uses CFL technology. The commercial CFL lights are ac powered and for dc operation with photo-voltaic energy, a new inverter design has been implemented. The inverter efficiency is better than 95% and the total harmonic distortion (THD) is less than 15%. The design incorporates SLA (Sealed Lead Acid) batteries for energy storage. The inverter is essential when hybrid operation (solar as well as ac line) is desired. For stand-alone solar application, it has been shown that the CFL lights can be directly operated from dc source and thus eliminate the inverter to minimize power losses. Further, a new dc operated ballast configuration was also investigated for CFL lighting to increase its luminous efficacy. The LED system employs pulse-width modulation technique controlled by a micro-controller for its operation. Both the systems incorporate a power management controller to adjust the lighting effect to compensate for weather conditions for days with inadequate solar charging. The two lighting systems have been deployed to illuminate two signs (Memphis and Remington Exit) on Interstate 40 East at the Remington exit. The CFL technology was used for the Remington Exit sign with a lighting area of 50-60 sq. ft. This report presents the design and development of the two systems, their outdoor deployment results, and recommendations for future research.

Table of Contents

I)	Introduction.....	4
II)	Solar Powered LED System.....	4
	1) LED Selection.....	4
	2) Solar Panel and Battery Selection.....	6
	3) LED Driver.....	7
III)	Solar Powered CFL System.....	7
	1) CFL Selection.....	8
	2) Solar Panel and Battery Selection.....	9
	3) CFL Driver.....	10
IV)	System Deployment.....	18
V)	Field Test Results	24
VI)	Further Explorative Research.....	30
	1) Commercial Ballast Operation with DC.....	30
	2) A DC Driven Modified Ballast for 26W CFL.....	34
VII)	Project Conclusion.....	37
VIII)	Research Publications Related to Project.....	39
IX)	References.....	39

I. Introduction

With energy costs rising and the high cost of running power lines to remote areas, there has been a growing interest in using renewable energy in low power highway applications. This project explores using photovoltaic solar panels to harness power from the sun to provide the required energy to illuminate overhead signs along the highways. There is 1000 Watts of power in one square meter of sunlight, but the typical solar panels of today can only collect 15% of that energy from the sun when operating into a matched load. This means a solar panel that has an area of one square meter can only collect 150 Watts out of 1000 Watts under ideal conditions. The inefficiency of the solar panel requires that the system efficiency must be at a maximum to reduce the size and cost of the solar panels.

The project looked at two approaches for formulating low cost reliable designs. One approach uses LED (Light Emitting Diode) technology and the second approach uses CFL (Compact Fluorescent Lamp) technology. Both approaches offer a high light intensity output with a minimum of input power. The main thrust of the research was to develop highly efficient driver circuitry in the effort to keep the solar panel size to a minimum. The specific goals of the research were:

- The drive circuitry should be as efficient as possible to minimize the required size of the solar panel.
- The overall electronic control system should be compact and portable.
- The lighting system must be of robust construction to handle the harsh environment along the highways.
- The lighting system circuitry should be robust, requiring a minimum of maintenance.
- System maintenance should require a minimum of effort.

II. Solar Powered LED System

The LED light system uses a PWM (Pulse Width Modulation) strategy for driving the two LED light fixtures. The PWM technique allowed for a minimum of power loss through a current limiting resistor. As long as the peak current and duration do not exceed the specifications of the LED, a low value current limiting resistor can be used, reducing power loss. The low value current limiting resistor was required because the battery voltage can be greater than 13V when fully charged, allowing for an over current situation, shortening the life of the LED's. The PWM strategy allows time-multiplexing and thus made it possible to drive the LED light fixture one at a time sequentially. For two LED lamps, the lamps not being on at the same time the peak current through the common line is one half and consequently the voltage drop is one half, reducing the power loss through lines powering the LED fixtures.

II. 1 LED Selection

With the recent advances in LED technology, white LED's seemed like a logical choice for the lighting system. Several types of high intensity white LED's under different

configurations were tested. After experimenting with up to 50 individual LED's mounted in an array, it was decided to use a single white LED light engine from Lamina. The LED engine utilizes Lamina's proprietary packaging technology that allows Lamina to densely cluster multiple LED's on a small substrate. This allowed for a high luminous intensity in a very small footprint. The LED engine footprint is 0.57" x 0.56". The plot in Fig. 1 shows the LED intensity as a function of the LED input current.

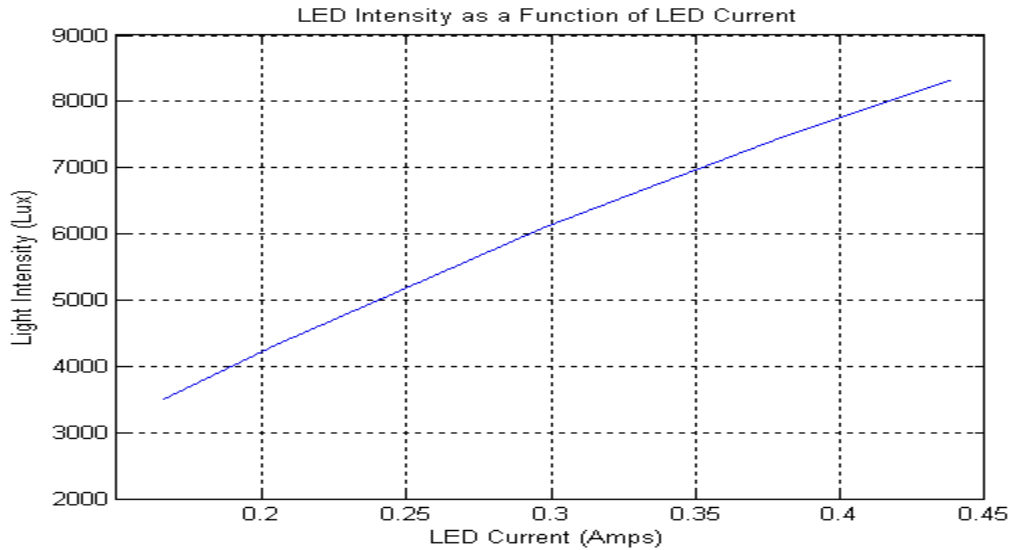


Fig.1 Plot – LED Intensity vs. LED Current

Mounting 50 individual LED's in an array would have required a printed circuit board to interconnect the LED's. Using the LED engine from Lamina allowed for a simplified and more compact design. The LED engine nominally dissipates 5 Watts of power, which requires the LED engine be mounted to a heat sink. Fig. 2 shows the completed LED light fixtures.



Fig.2 LED Light Fixtures

II. 2 Solar Panel and Battery Selection

Two types of batteries were tested in the lab, lithium-ion and lead acid. Lithium-ion batteries are light weight with high capacity, but very sensitive to their charging and can be damaged easily by applying an over voltage or allowing them to discharge below its rated minimum voltage. Typical lithium-ion battery chargers provide a constant voltage and constant current source. As the battery reaches full charge and the charging current drops to within 3% of the 1C rating of the battery, the charger must disconnect from the battery, because trickle charging causes permanent damage to lithium-ion batteries. Using a lithium-ion battery would require specialized circuitry to ensure the proper charging characteristics. The charging requirements for a lead acid battery are more forgiving than those of a lithium-ion battery and there are numerous ‘off the shelf’ solar controllers for interfacing between solar panels and lead acid batteries that prevent over charging. Because of cost considerations, its long life, wide operating temperature range, and ease of charging, a 12V 20Ahr sealed lead acid battery was chosen.

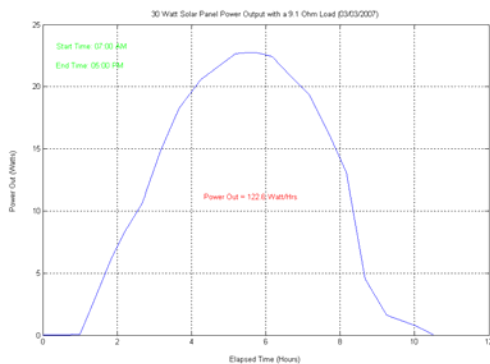


Fig.3a - Resistive Load

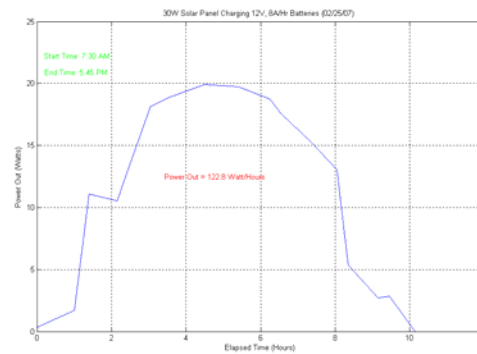


Fig.3b – Charging 12V Battery

In early March 2007, testing was done with two 15W solar panels connected in parallel to make a 30W panel. Since solar panels are most efficient when the rays from the sun are normal to the surface of the panel, the panels were placed at a 30-degree angle with the horizon facing south. In one test, the solar panel output power was measured with a matching resistive load connected to the panel. Figure 3a shows the output power into the matched resistive load as a function of elapsed time. The second test was conducted with three fully drained 12V 8Ahr SLA batteries connected in parallel at the solar panel output (see Fig. 3b). In both cases, under ideal sunny conditions the panels were able to harness 120 Watt-hrs of energy in a ten-hour period. The plots reflect a peak charge time of approximately 3.5 hours.

Each LED lamp nominally requires 5W for a total of 10W, assuming that two LED lamps will be used. With 120 Watt-hrs of stored energy, this would allow for a 12 hour run time. One should expect the lights to be on for a 12-hour period during the winter months. Allowing for less than ideal conditions for harnessing sun’s energy, especially during the winter months, an additional 15W panel was added to give a total of 45W. This gives a factor of 1.5 over the minimum requirement.

II. 3 LED Driver

Figure 4 below shows a simplified block diagram of the LED driver circuit. The driver includes a power latch circuit, PIC control circuit, and a pair of MOSFET switches that turn on the LED's. A power latch circuit was used to provide a reliable master reset pulse for the PIC micro controller and provide an easy way to re-initialize the PIC if control of the program is lost. The PIC output controls when the lights turn on and provides the PWM signals that control the manner in which the lights turn on. The MOSFET switches close the path for the LED lamps allowing them to turn on. A phototransistor was used to detect when the lights should turn on and off. Using the solar panel to detect when the lights should turn on proved to be unreliable because the solar panel output voltage varies under different loading conditions and leakage through the solar controller caused a voltage to appear across the solar panel at night, preventing the lights from turning on.

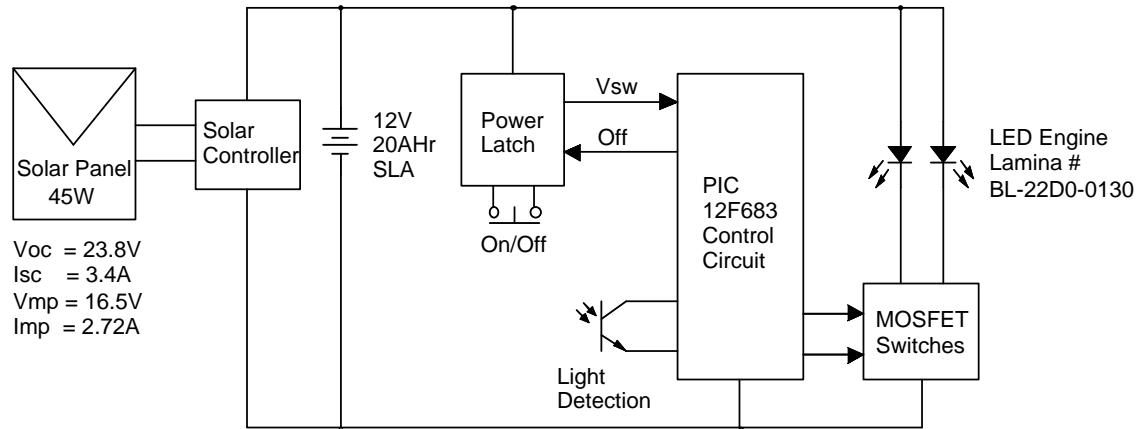


Fig.4 LED System Block Diagram

Using its A/D feature the PIC micro controller monitors the phototransistor voltage and determines whether to turn-on or turn-off the lights. The programming code provides hysteresis to prevent the lights from oscillating 'on and off' when at the phototransistor voltage is at its threshold. When the lights are on, the PIC provides two 1KHz square waves that are 180 degrees out of phase for turning the lights on. The timing signals being 180 degrees out of phase means that only one light is actually on at a time, although this is not transparent to the motorists' eyes. The PIC also continuously monitors the battery voltage. Should the battery voltage drop below 10.5V, the PIC will turn off the lights. To prevent the lights from oscillating on and off, the programming code provides hysteresis that prevents the lights from turning back on until the battery voltage climbs back to 11.25V. The PIC can also detect a failure with the solar controller or an open fuse, which would prevent the solar panel from charging the battery. If the battery voltage drops below 9V, the PIC will send a signal to the power latch that turns power off to the system, preventing over discharge of the battery. A failure of this type would require that a technician troubleshoot the system and replace the failed component, then re-initialize the system through the power latch circuit.

Figure 5 below shows a detailed schematic of the LED driver circuit.

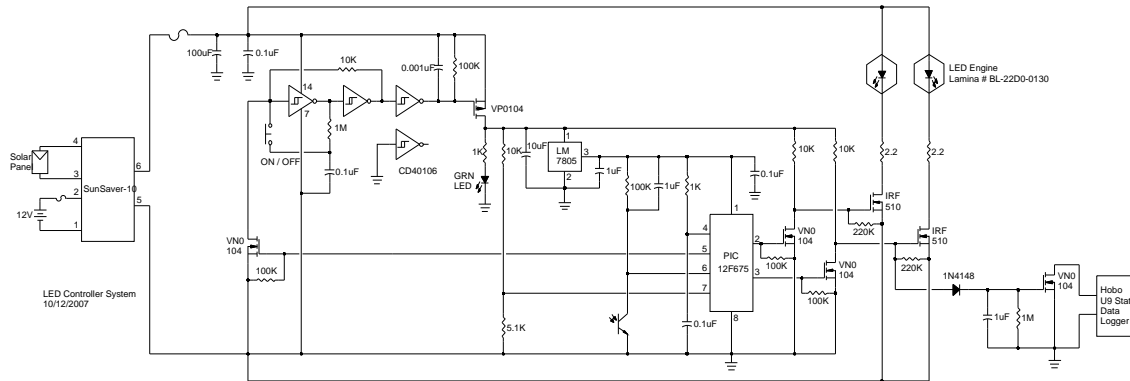


Fig.5 LED Driver Schematic

III. Solar Powered CFL System

With recent advances in compact fluorescent lamps, CFL technology appeared to be a logical choice for consideration in this project. Today's compact fluorescent lamps come in a wide variety of shapes and sizes. The lamps offer enhanced brightness with a greatly reduced input power requirement. For example, a 14W CFL can give the equivalent light output of a 65W incandescent lamp and have an eight-year life. CFLs require a ballast to turn on the lamp (provides a high voltage) and once 'ignited' the current through the lamp drops. Many CFLs available today come with the ballast as an integral part of the lamp, which allows them to be used in standard light fixtures.

Unlike LED's though, CFLs require a high voltage of 100 to 120Vrms. Since it was desirable to have a 12V system that allowed the use of a standard 12V solar panel, a high voltage inverter would need to be developed. A large portion of the project was spent developing a high-efficient DC to AC inverter with a low harmonic content. The experimental results of this research have been disseminated through five publications in IEEE International Conferences and Symposiums.

III. 1 CFL Selection

Several types of compact fluorescent lamps were tested in the lab. In choosing the number of lamps, the style of lamp, and the lamp power, the following factors were considered:

- Require sufficient brightness with uniform illumination for the entire 15 ft X 9ft sign
- Desirable that lamp can be mounted in a standard weather proof light fixture
- Use low wattage lamps to keep solar panel size to a minimum

CFLs in a standard floodlight packaged provided the best uniform coverage of light. The CFL floodlights come with the electronic ballast as an integral part of the lamp, allowing them to be used in a standard screw-in floodlight fixture as shown in Fig. 6. The 8W

CFLs are equivalent to a 40W incandescent lamp and give an output of 375 lumens. A minimum of 3 lamps was required to give complete coverage of the sign, for a total power requirement of 24W.



Fig.6 CFL Light Fixtures

III. 2 Solar Panel and Battery Selection

As with the LED system, Sealed Lead Acid (SLA) and lithium-ion batteries were considered for the project. In the end, SLA batteries were chosen because of cost considerations, their long operating life, wide operating temperature range, and ease of charging. Twelve 12V batteries are used to obtain a peak output voltage of 144V. Initial experimentation was done using three 12V 8Ahr batteries along with a DC/DC converter to obtain a 144V output, but there was undesirable power loss using the DC/DC converter. Using the twelve batteries in series eliminated the power loss associated with the DC/DC converter. The inverter current requirement was approximately 200mA with a 25W output load. The batteries chosen have a 3.4Ahr rating that will allow for a 17 hour run time before recharging is necessary and still allow for a compact design.

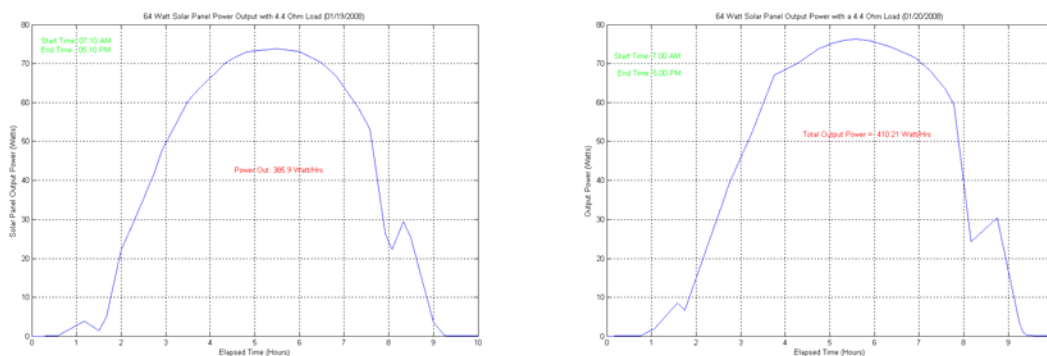


Fig. 7 Output Power Characteristics of 64W Solar Panel

In January 2008, two tests were conducted with a 64W solar panel with a matched resistive load connected to its output to quantify the solar panel's power output during a typical winter day in Arkansas. The solar panel was rated to have a short circuit current

of 4.8A and an open circuit voltage of 23.8V. The solar panel has an output current of 3.88A at 16.5V when it is operating at its maximum power. In the effort to achieve maximum power transfer during the test, a 4.2ohm resistor was connected to the solar panel output to match the panel's output impedance at maximum power. The first day's testing was conducted with the panel set at a 34.5-degree angle to the horizon (see Fig. 7, plot on left) and the second day's test was conducted with the panel at a 58.2-degree angle (Fig. 7, plot on right). The weather was clear and sunny for both tests. The solar panel harnessed 385Whrs of energy with panel at a 34.5-degree angle and 410Whrs with the panel at a 58.2-degree angle. There was about a 6% improvement with the panel angle set at 58.2-degrees and both plots reflect a peak charge time of approximately three hours.

Each CFL lamp nominally requires 8W for a total of 24W, assuming that three CFL lamps will be used. With 385Whrs of stored energy, this would allow for a 16-hour run time. One should expect the lights to be on for a 12-hour period during the winter months. This gives a factor of 1.33 over the minimum requirement, allowing for less than ideal conditions during overcast days.

III. 3 CFL Driver

Various pulse width modulation (PWM) approaches were investigated for the development of the high voltage DC/AC inverter. A novel sectionalized PWM (S-PWM) multilevel strategy was developed through the project research. The new S-PWM approach was introduced at the IEEE International Symposium on Circuits & Systems in May, 2008 in Seattle, Washington [1].

Modern inverters employ some form of pulse width modulation (PWM) that allows easy control of output ac power [2]. The most common PWM is the sine-triangle PWM (SPWM) where a reference (desired) sinusoid is compared against a triangular carrier to produce the PWM switching signal. Fig. 8a shows the basic SPWM topology and the generation of SPWM signal in Fig.8b. Fig.9 on the following page shows the frequency spectra of the SPWM signal for even multiple of the reference signal with a modulation depth $m=0.8$ (m is the ratio of control voltage peak to that of triangle).

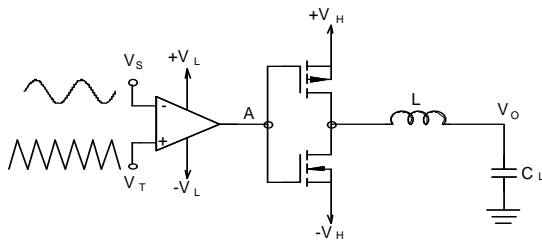


Fig.8a Basic SPWM Topology

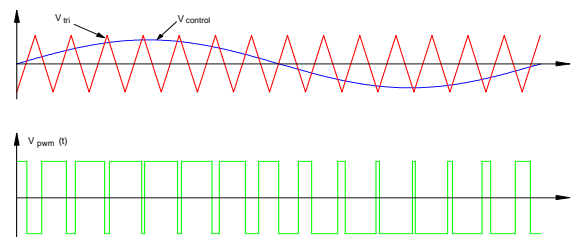


Fig.8b Sine Triangle PWM (SPWM)

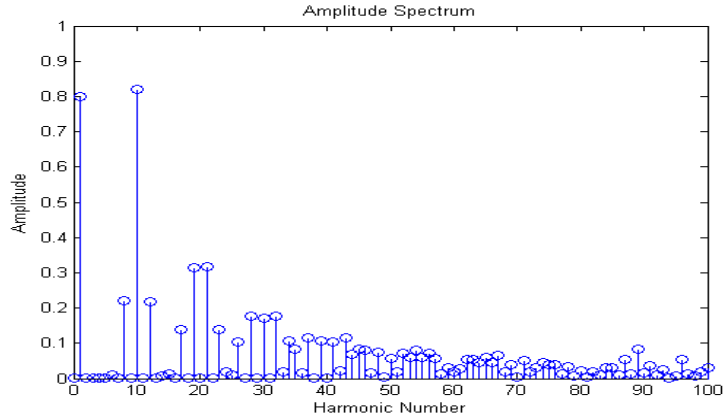


Fig.9 SPWM Spectra

As observed from Fig.9, the effect of SPWM is to move the harmonic frequencies away from the reference signal. To avoid carrier sidebands falling below the fundamental component, a frequency ratio of 10:1 or better is recommended [2, 3]. A low pass filter can eliminate the high frequency components, and the resultant filter output is the reference signal with higher amplitude determined by the H-Bridge bus voltage. Closed loop feedback can be employed in the configuration to improve load regulation and reduce THD. Since PWM operates in the switch ‘on’ and ‘off’ mode, it provides an efficient means of power transfer, and thus SPWM technique, in general, is attractive for dc-ac conversion. However, its efficiency can be improved by reducing harmonic contents and the switching losses incurred in the ‘on’ resistance of the drive transistors.

With harmonic elimination as the major focus, various modulation methods have been proposed in the literature for the design of multilevel converters: Space vector control, selective harmonic elimination method, space-vector PWM, and multi-carrier SPWM [4]. Multi-carrier SPWM is very popular in industrial applications and they generally employ either carrier disposition technique or phase-shifted carrier method [5]. In this project, a new multilevel strategy was developed where the reference sinusoid is split into sections and each section is carrier modulated with a constant modulation index. The number of sections depends on the number of levels desired on the multilevel output.

The primary goal of the multilevel inverter is to produce a high voltage waveform that closely approximates a sinusoid. A close examination of the 2-level SPWM technique (Fig. 8b) shows that the H-Bridge switches operate through the entire high voltage range ($\pm V_H$) irrespective of the sine wave amplitude level. This causes unnecessary switching losses that can be reduced if the reference signal is split into sections and PWM is produced for each section using the conventional triangular carrier. The concept is illustrated in Fig 10 and Fig. 11 for a two-section modulation.

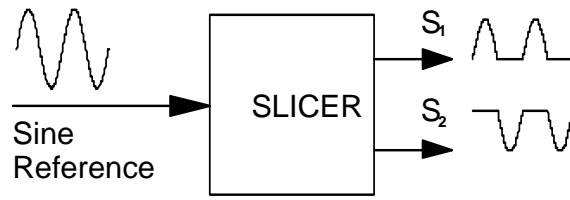


Fig.10 Slicing Reference Signal into Two Halves

Fig.10 shows the splitting of the reference signal into two segments S_1 and S_2 . These two sections are fed into the SPWM block in Fig.11 and the sliced segments are carrier modulated by the high frequency triangular wave. Two low voltage PWM signals appear at the output of the SPWM block. These PWM signals are level shifted in the ADM (Amplitude Division Multiplexing) block (two levels in this case) and the output is filtered to produce the high voltage signal [6].

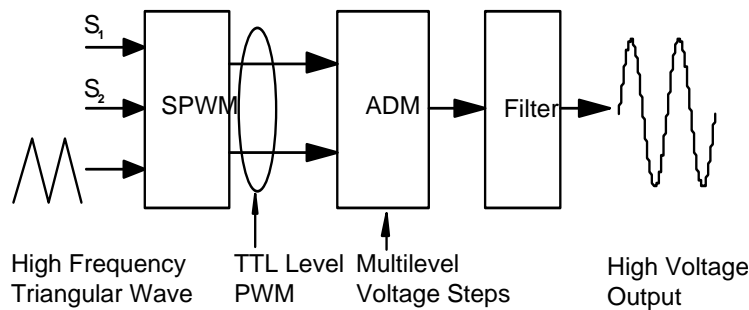


Fig.11 Multilevel SPWM Scheme

Extensive simulation studies were carried out using MatLab to evaluate the effectiveness of the new modulation strategy. Throughout the simulation studies, the reference signal frequency is 60Hz and the carrier frequency is 600Hz with a modulation depth m of 0.8. S-PWM refers to Sectionalized PWM. The simulation results, shown in Figures 12a – 12d, employ four equally divided sections of the reference sinusoid along with two carriers that are 180° out of phase.

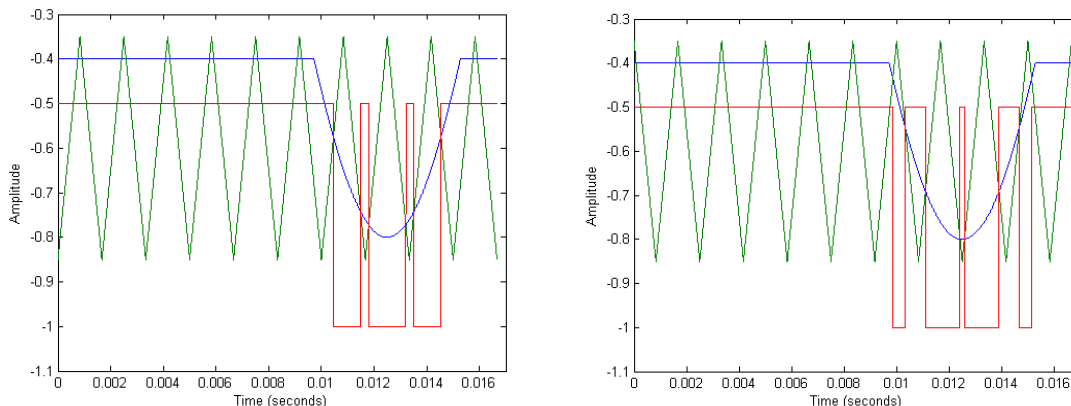


Fig.12a Sectionalized PWM of Section 1 (0° & 180° Carrier)

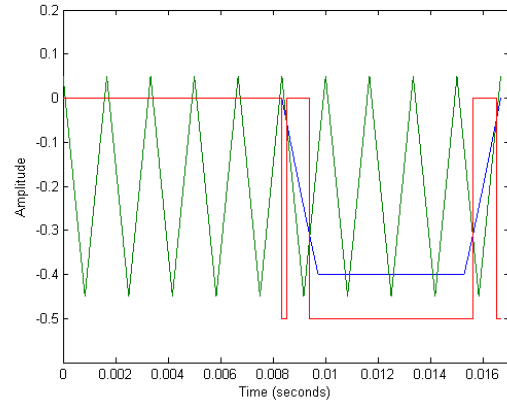
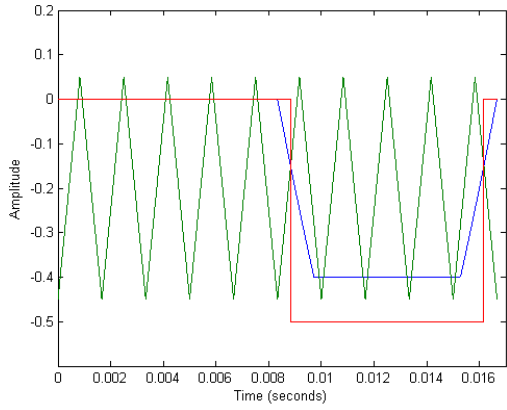


Fig.12b Sectionalized PWM of Section 2 (0° & 180° Carrier)

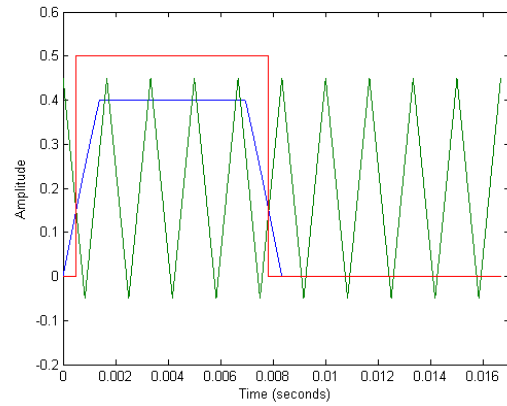
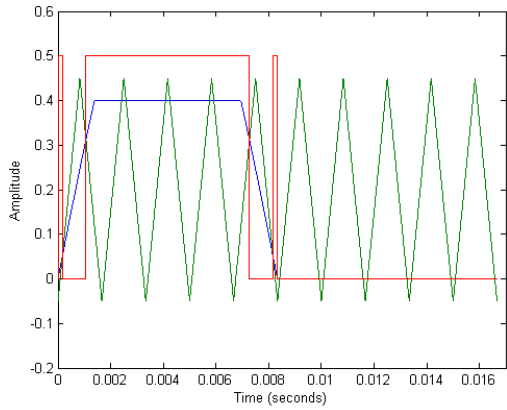


Fig.12c Sectionalized PWM of Section 3 (0° & 180° Carrier)

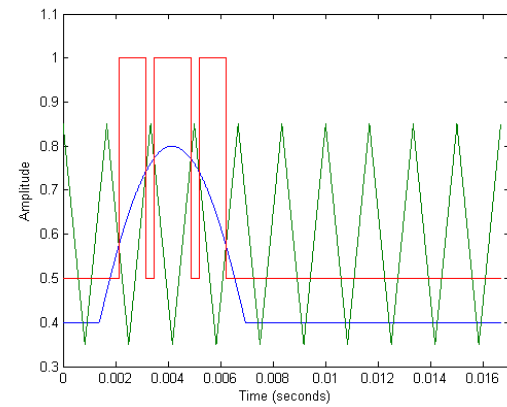
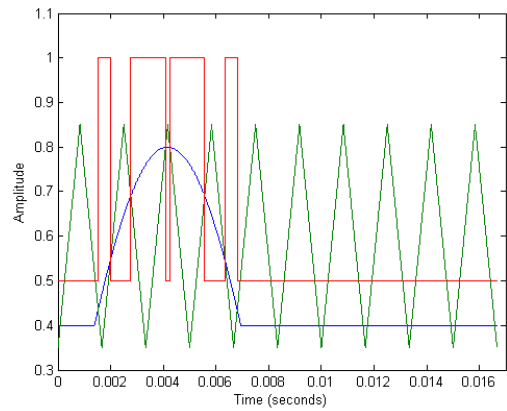


Fig.12d Sectionalized PWM of Section 4 (0° & 180° Carrier)

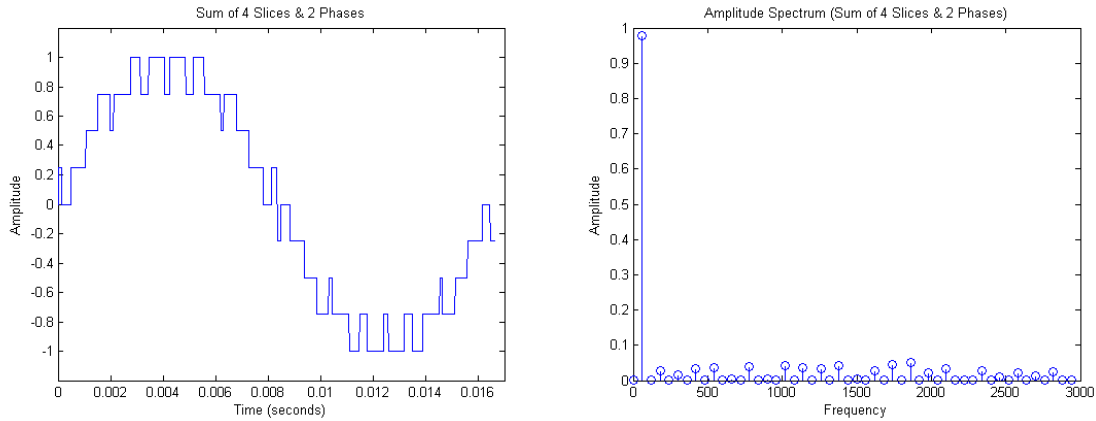


Fig.13 Simulated S-PWM of 4 Sections & 2 Phases (THD = 14.53%)

The overall S-PWM of four slices and two phases is obtained through summing of the individual PWM signals. The resulting S-PWM signal is shown in Fig. 13, along with its frequency spectra. The simulation results show a total harmonic distortion (THD) of 14.53%. A detailed discussion on Sectionalized PWM can be found in reference [1].

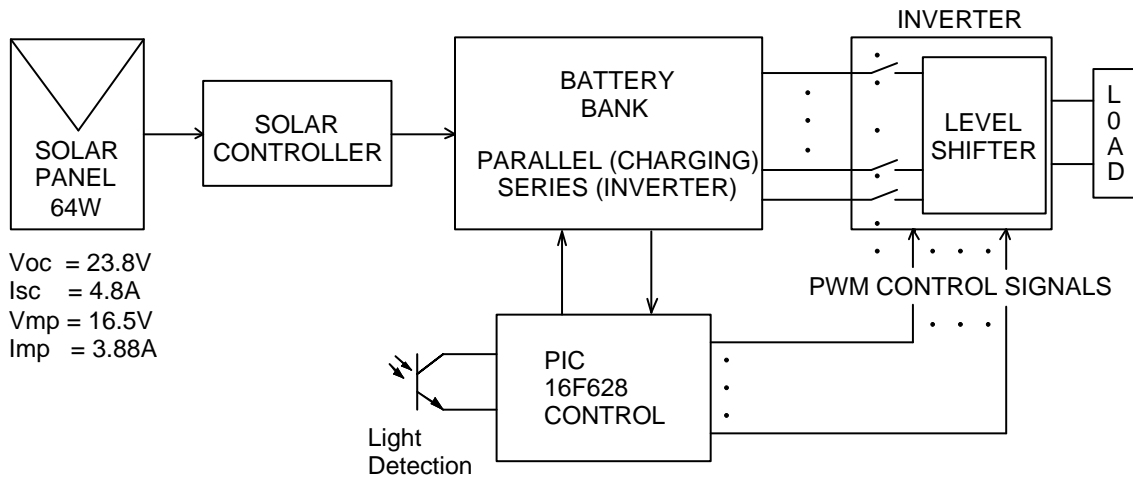


Fig.14 CFL System (DC/AC Inverter) Block Diagram

Fig. 14 shows the functional block diagram for CFL system. The system includes a 64W solar panel with a solar controller, battery bank switching circuit, level shifter (ADM) circuit, and PIC micro controller. The PIC 16F628 micro controller is the heart of the system and provides the required timing for generating the S-PWM signal. The PIC continuously monitors the ambient light and determines when the inverter should turn the CFL lamps on or off. The PIC also monitors the system voltage and turns off the inverter if the voltage drops below 10.5V. During the day, PWM control signals from the PIC switch the inverter off and connect the batteries in parallel so the 12V solar panel can charge all of them. Hysteresis is provided in the PIC programming code to prevent the system from oscillating on and off when the voltage from the light detection circuit is at the transition level. When the PIC determines that it is dark outside, control signals from

the PIC switch the twelve 12V batteries in series. Lines from the battery bank provide the voltage steps (0V, 36V, 72V, 108V, 144V) for the level shifter (ADM). The low voltage PWM control signals are level shifted to the appropriate voltage in the level shifter (ADM) circuit to produce the S-PWM signal. The level shifting occurs in increments of 36V. An integral part of the level shifter circuit is an H-bridge to provide the negative portion of the output signal.

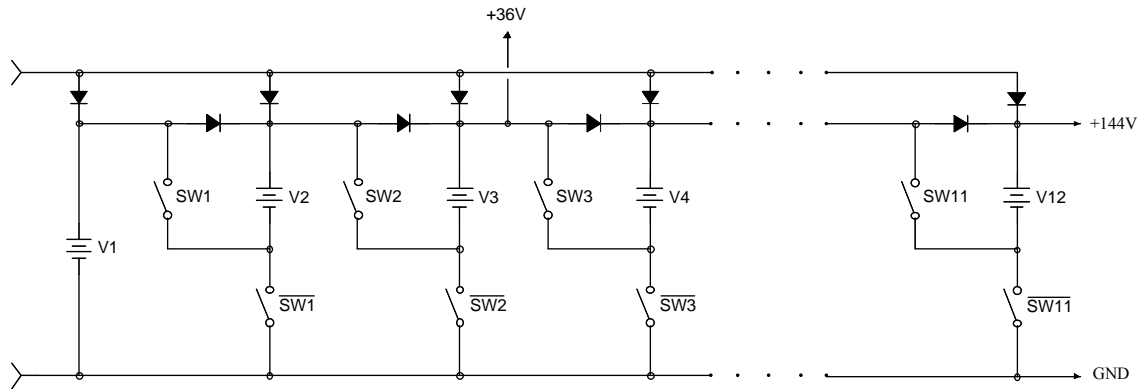


Fig.15 Battery Bank Switching Diagram

A simplified schematic of the battery bank circuit is shown in Fig. 15. The PIC micro controller monitors the voltage from the light detection circuit and controls when the switches are opened or closed. When lower switches SW1' – SW11' (denoted with a top bar in schematic) are closed, and upper switches SW1 - SW11 are open, the batteries are placed in parallel allowing them to be charged by the solar panel (day time). Each battery is protected with a current clamp circuit to prevent the initial charging current from being greater than 1.3A. The twelve batteries are in series when switches SW1 - SW11 are closed and SW1' - SW11' are open (SW1' implies it is complement of SW1). Five lines tap out of the battery bank to provide the level shifter with the needed voltage levels (0V, 36V, 72V, 108V, 144V) when the batteries are in series. Fig. 16 shows the pc board for series-parallel conversion of battery bank.



Fig. 16 Battery Bank PC Board

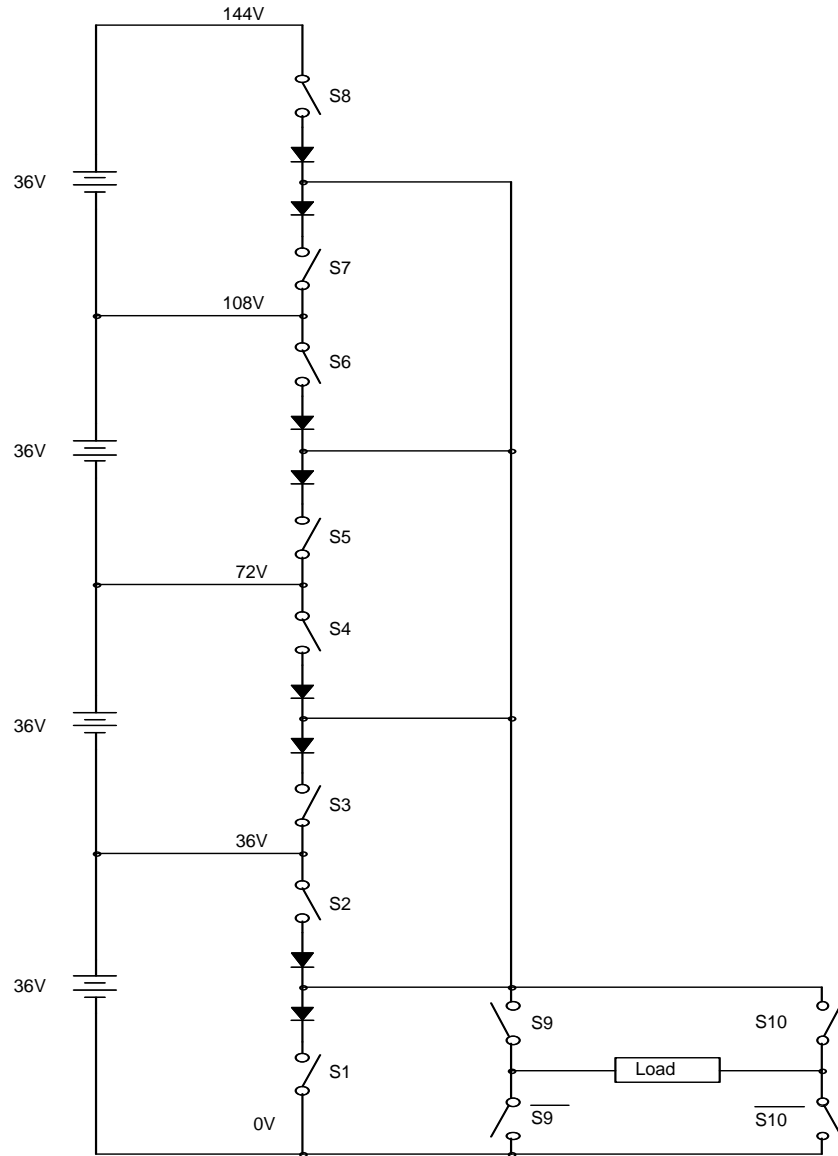


Fig.17 Level Shifter

The topology of the level shifter is shown in Fig. 17. The PIC controls the timing of the switches. Switches S2, S4, S6, and S8 are used to raise the output voltage to the next higher voltage (positive going slope of sine wave). Switches S1, S3, S5, and S7 are used to pull the output voltage down to the next level (negative going slope of sine wave). The switching is implemented with n-channel and p-channel MOSFETs. Using both n & p-channel type MOSFETs makes the inverter capable of driving capacitive loads. Switches S9, S9', S10 and S10' make up the H-bridge. During the first half of one cycle S9 and S10' are closed while S9' and S10 are open. The second half of the cycle S9' and S10 are closed while S9 and S10' are open. The use of the H-bridge made it possible to achieve a 288Vpk-pk output voltage with only twelve 12V batteries. Careful attention must be paid to insure non-overlapping control signals to avoid shoot through.

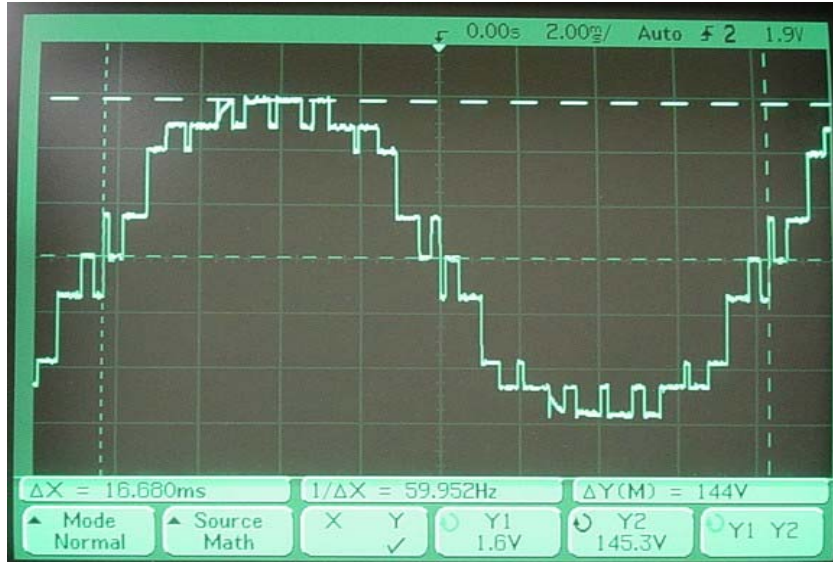


Fig.18 Experimental S-PWM

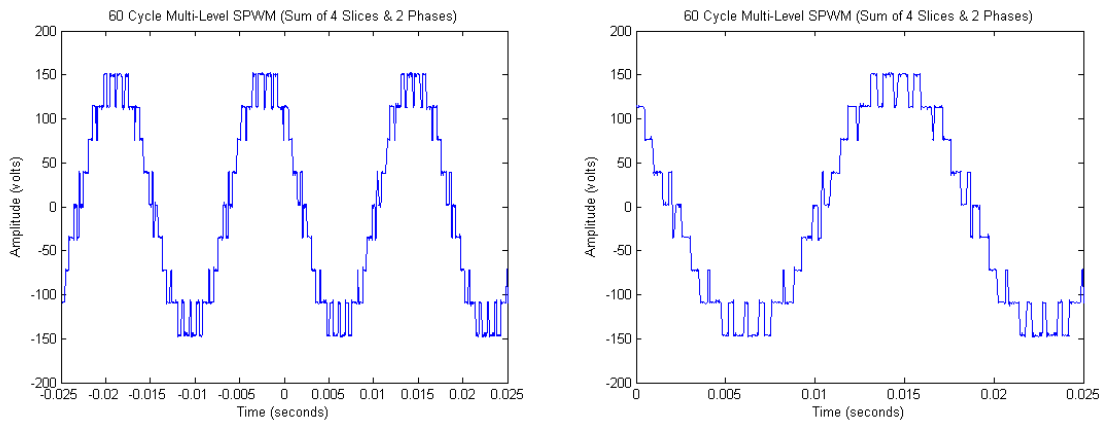


Fig.19 Experimental S-PWM – Captured on DOS & Plotted in MatLab

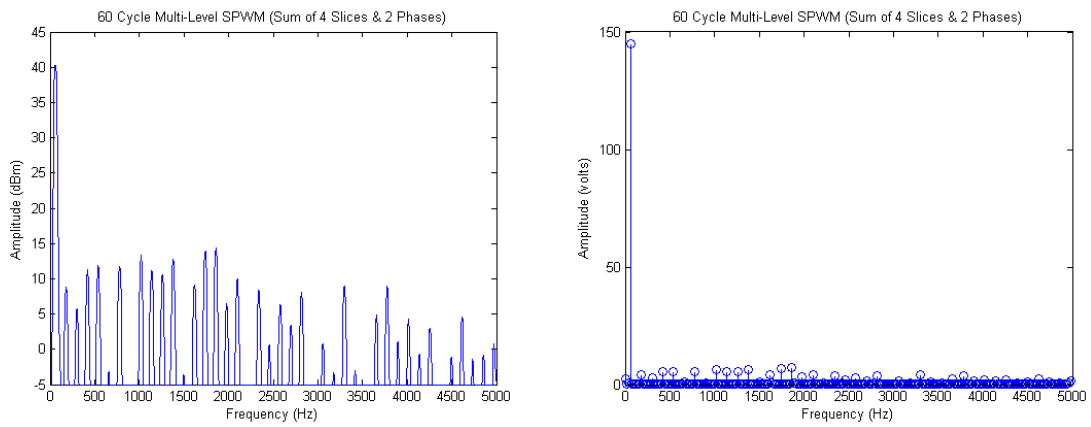


Fig.20 Frequency Spectra of Experimental S-PWM (THD = 14.54%)

The experimental S-PWM signal under load is shown in Fig. 18. The S-PWM signal was captured on a digital oscilloscope while driving the 14W compact fluorescent lamps. The measured frequency and amplitude are 59.95Hz and 144Vpk respectively. The experimental S-PWM data was captured on a digital oscilloscope and transferred to MatLab for FFT analysis (Fig. 19 & Fig. 20). The frequency spectra are shown in Fig. 20, where it can be seen that the harmonic components of the experimental signal are at least 30dB below the fundamental frequency. The measured total harmonic distortion was 14.54%, matching the simulated THD of 14.53%.

IV. System Deployment

The two lighting systems (LED and CFL) were deployed at the Remington Road exit in the eastbound lane of Interstate 40 at mile marker 169. System deployment was completed in several stages, as different parts of each system were made ready. Several factors made this a suitable site to deploy the lighting systems.

- The site location is away from city lights that would make it difficult to evaluate the effectiveness of the lighting system
- There was a relatively clear view to the south for the solar panels
- Existing light fixtures and conduit at the site provided platform for mounting the new lights.

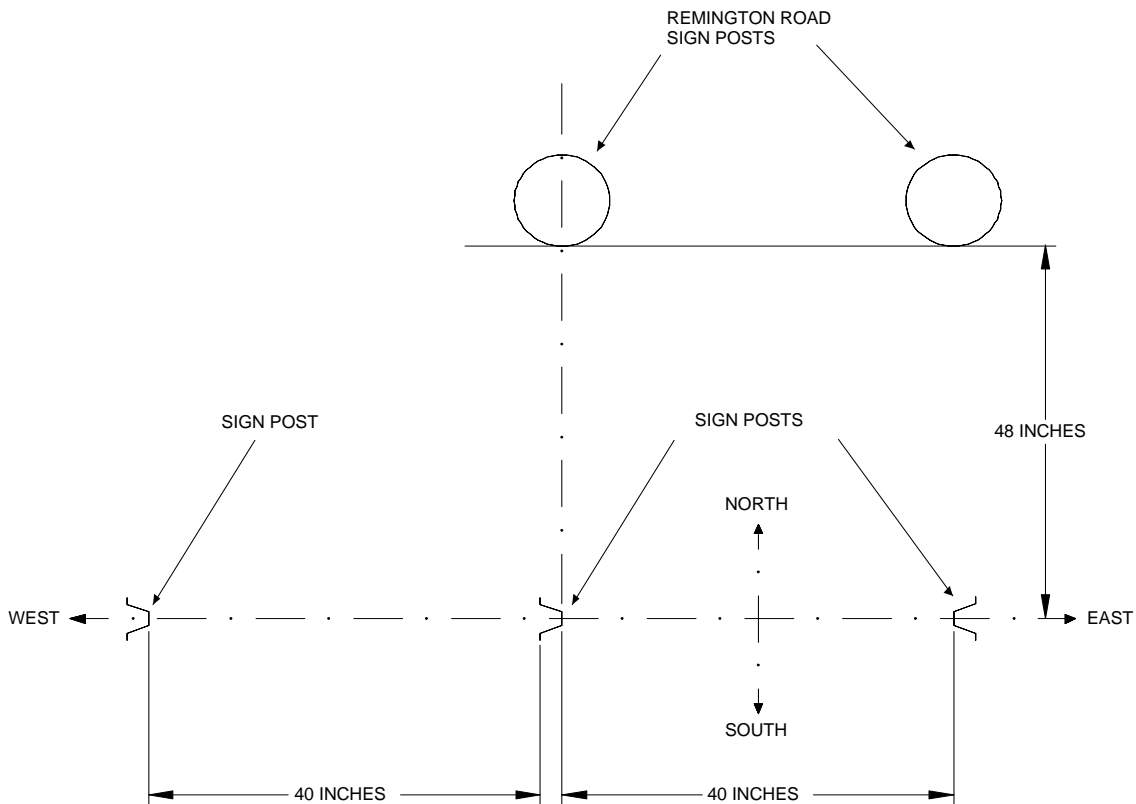


Fig.21 - Top View – Post Placement for Solar Panels & Control Boxes

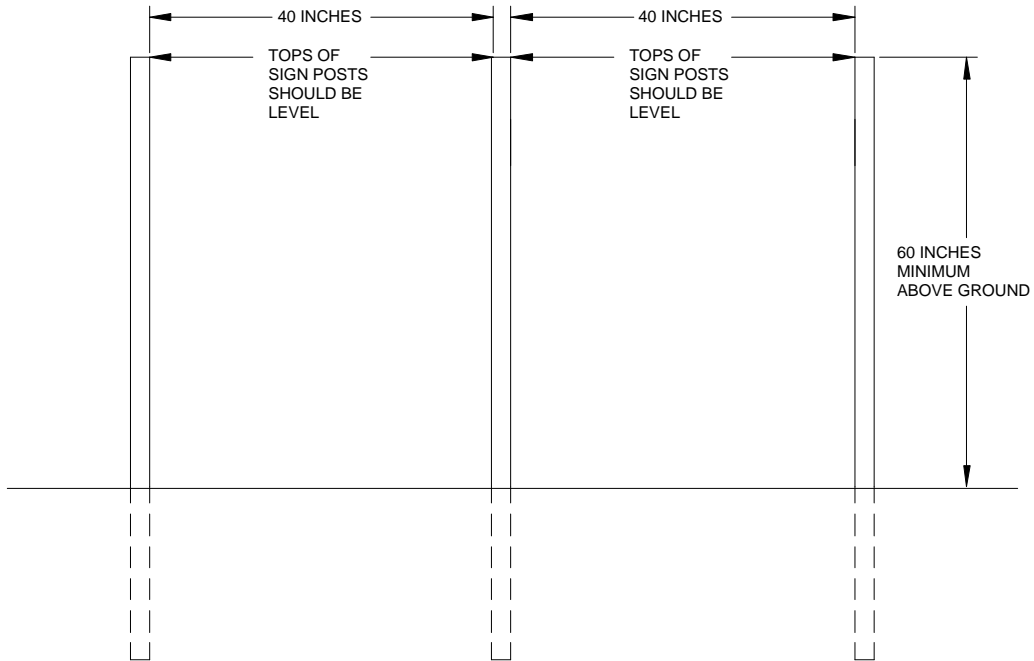


Fig.22 – Front View – Post Placement for Solar Panels & Control Boxes

Three posts were driven in the ground to provide a structure to mount the solar panels (Fig 21 & Fig. 22). Steel frames were welded together to support the solar panels and are designed in a way that allows adjustment of the angle of each solar panel. The solar panels are mounted at a 34.5° angle to the horizon, facing south. This angle places the solar panel midway (Fig. 23) between the peak angle of the sun on June 21st and December 21st.

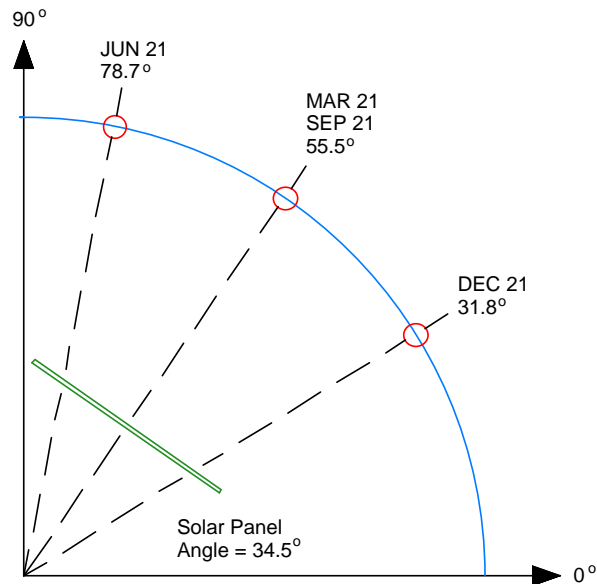


Fig.23 Solar Panel Orientation



Fig.24 Installation of CFL Control Box (Late June 2007)

The CFL solar panel and CFL control box were mounted in late June 2007. The solar panel shown in Fig. 24 is a 45W panel. The 45W solar panel was initially used for the CFL system until shipment of the 64W panel was received. Using the 45W panel allowed testing of the CFL system to begin. The 45W panel was later moved and installed with the LED system. The wires powering the CFL lamps were placed in flexible conduit and buried in a shallow trench under the ground. The project PI is shown digging the trench for the conduit. The conduit routed to the base of the Remington Road signpost.



Fig.25 Preparing to Install CFL & LED Light Fixtures (Mid-July 2007)

Installation of the light fixtures was completed in mid-July (Fig. 25). Installing the light fixtures involved blocking one lane of traffic on Interstate 40 so that AHTD personnel and equipment could move into place to hang the new light fixtures. The existing conduit was used to run new wires for the light fixtures and the existing light mounting unit was used as a platform to set up the new fixtures. After three CFL light fixtures were mounted at the Remington Road exit sign, equipment and personnel were moved to the left lane to hang two LED light fixtures at the 40 East Memphis sign.



Fig.26 Gutting Existing Light Fixtures

In Fig. 26, the principal student and AHTD electrician are shown gutting the existing light fixtures. The plexi-glass covers, fluorescent bulbs, and ballasts were removed from the existing platform. The old wiring was pulled out to make room for the new wires. The existing fixtures extend out approximately four feet below the signs and provided an excellent platform for mounting the new system.

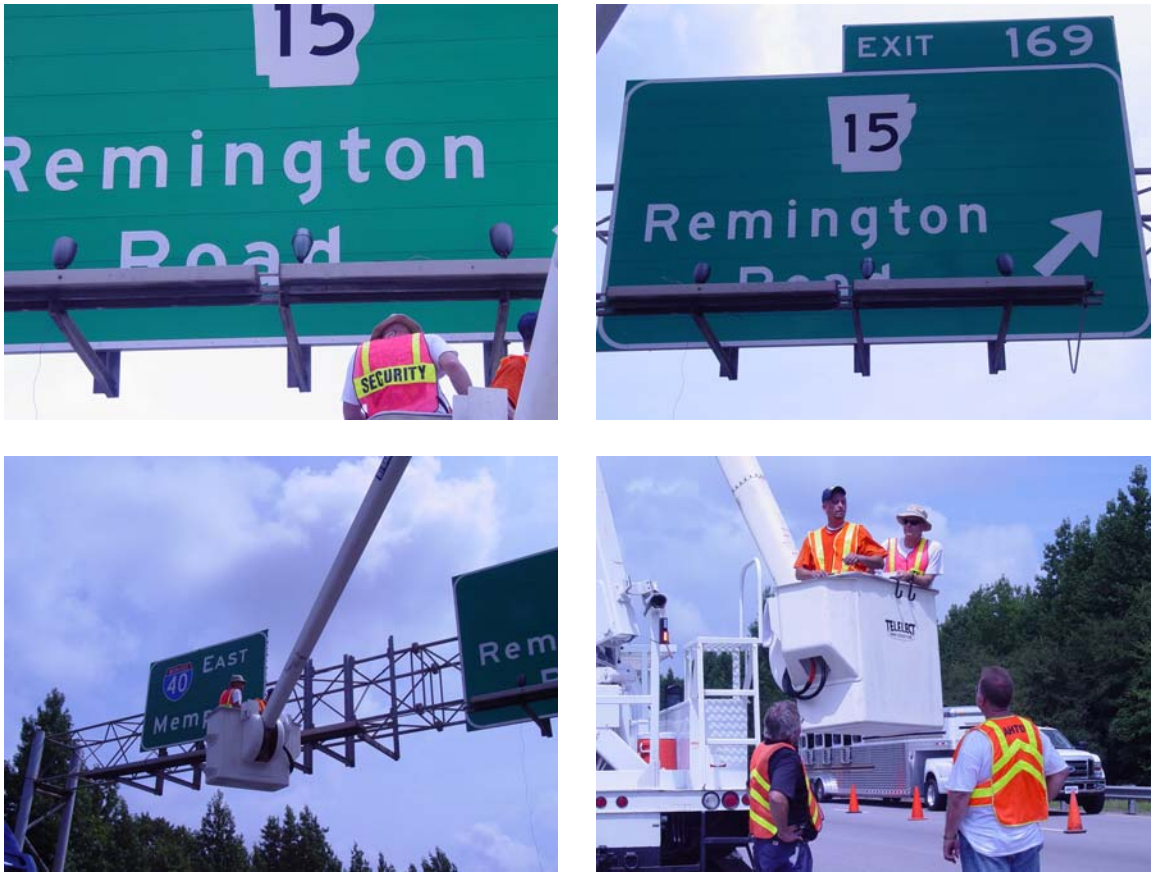


Fig.27 Installation of New CFL Light Fixtures

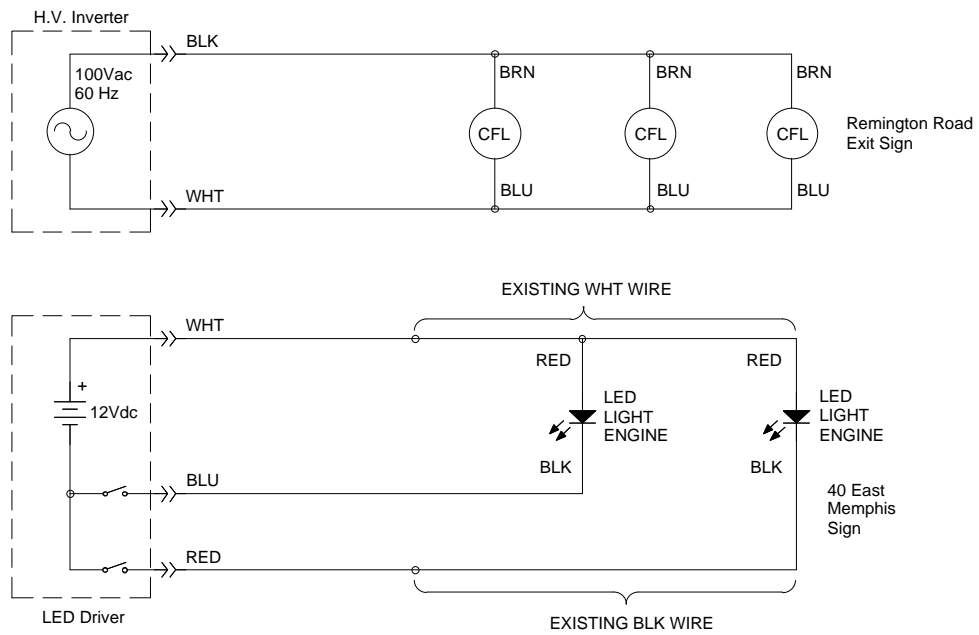


Fig.28 Remington Road Wiring Diagram

The placement of the three CFL lights is shown in Fig. 27. The light fixtures were mounted to watertight terminal boxes, where splices were made to connect power to the lamps. Self-tapping screws through mounting tabs on the terminal boxes secured the light fixtures to the existing platform. Fig. 28 shows the wiring diagram for the CFL and LED systems.



Fig.29 Installation of LED Control Box (Mid-September 2007)

The LED control box and solar panel were installed in mid-September. The top left picture in Fig. 29 shows a T-box that was installed to accommodate the wires from the LED driver to the LED lamps. The top right picture in Fig. 29 shows the LED control box that holds the LED driver circuit, 12V 20Ahr battery, and solar controller for the LED system. The lower left picture shows the CFL control box, containing twelve 12V 3.4Ahr batteries and the CFL driver circuitry. Both systems use rugged steel weather resistant boxes to house the batteries and circuitry, and are locked with padlocks to discourage tampering.



Fig.30 LED System & CFL System (January 2008)

The pictures in Fig. 30 show the lighting systems in their current configuration. The LED system is on the left with the 45W solar panel and the CFL system is on the right with the 64W solar panel. Keeping the solar panels and control boxes close to the ground has made the lighting systems accessible to data collection and maintenance. Construction of the structure has proved to be rugged. The structure recently survived a windstorm with wind gusts of more than 50 miles an hour.

V. Field Test Results

The LED driver circuitry has proven to be efficient and reliable. Measurements taken in the lab have shown an efficiency of 98% with an output load of 10W (Fig. 31). There have been no field failures with the LED driver.

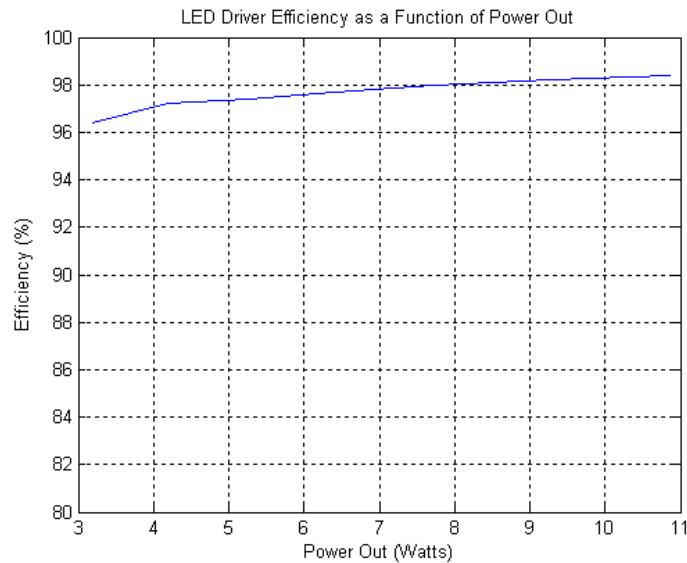


Fig.31 LED Driver Efficiency

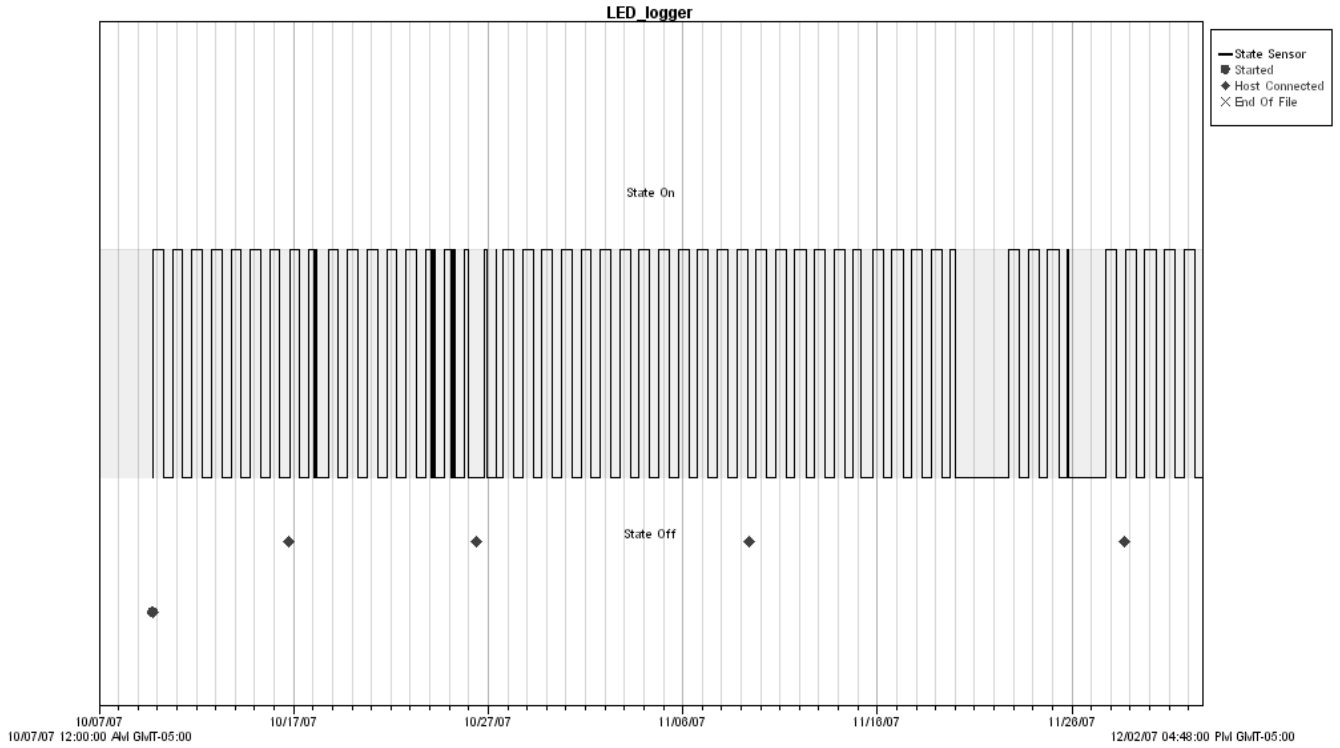


Fig. 32 LED Data Logger – Data Set 1

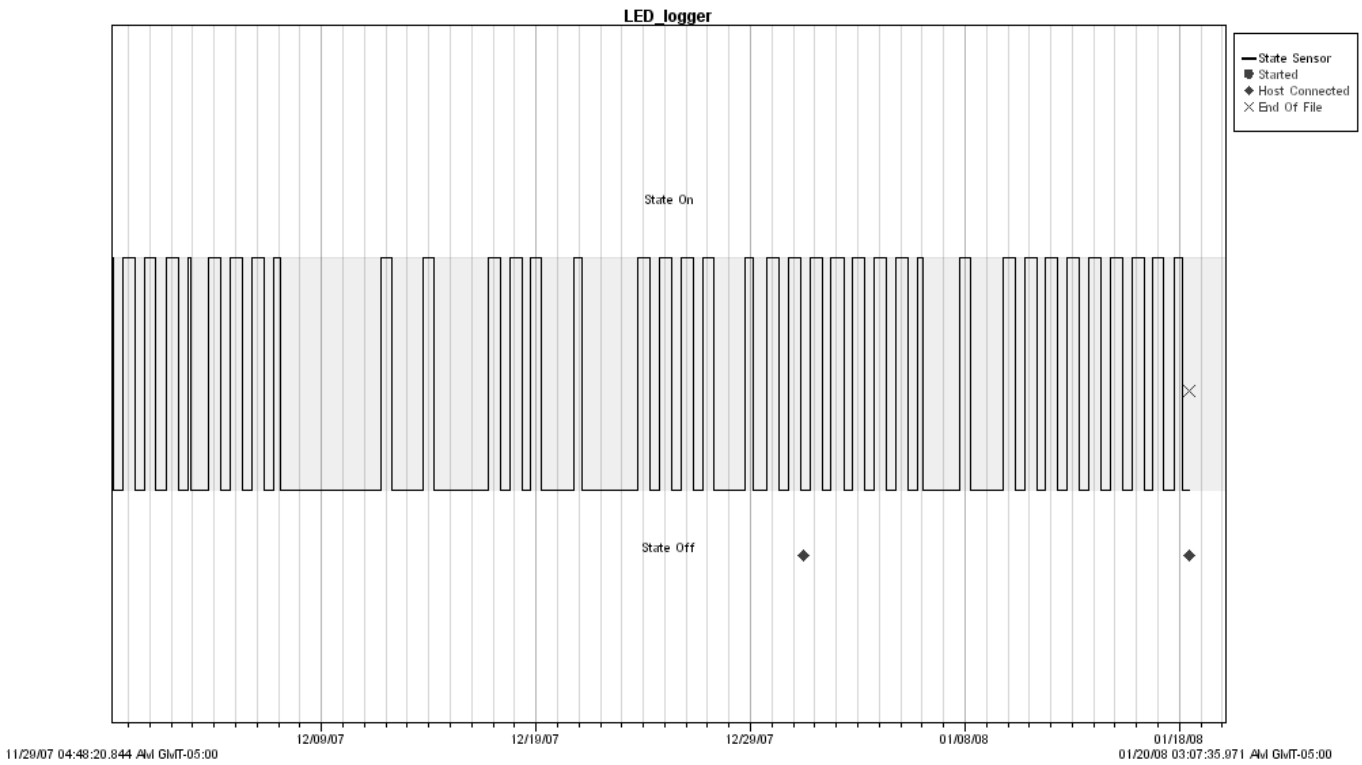


Fig. 33 LED Data Logger – Data Set 2

Each lighting system has a data logger that monitors and records when the lights transition on and off. Use of the data loggers has been a useful troubleshooting tool. The plots in Fig. 32 and Fig. 33 show the LED light on and off times from October 10th to January 18th. In early October the lights typically turned on at 7:00PM and turned off at 7:00AM. The plot in Fig. 33 shows a case where the lights turn on at approximately 6:30PM and turn off at 8:00AM. On October 25th and 26th, the data shows that the lights oscillated on and off several times during the night. Adjusting a value in the PIC programming code that added additional hysteresis to the low voltage cutoff circuit rectified this problem.

There are times when the lighting system did not harness enough energy for the lights to stay on all night and there are several days in December and January when the lights did not turn on at all. Heavy cloud cover was a factor during the periods that the lights did not stay on all night or did not turn on at all. Unfortunately, the solar panels are also catching some shade in the afternoons. During the winter months when the sun is low in the sky, a shadow is being cast on the solar panels from the tree line just south of the solar panels. This situation is expected to improve as we enter spring and the sun rises higher in the sky, causing the shadow from the tree line to become shorter.

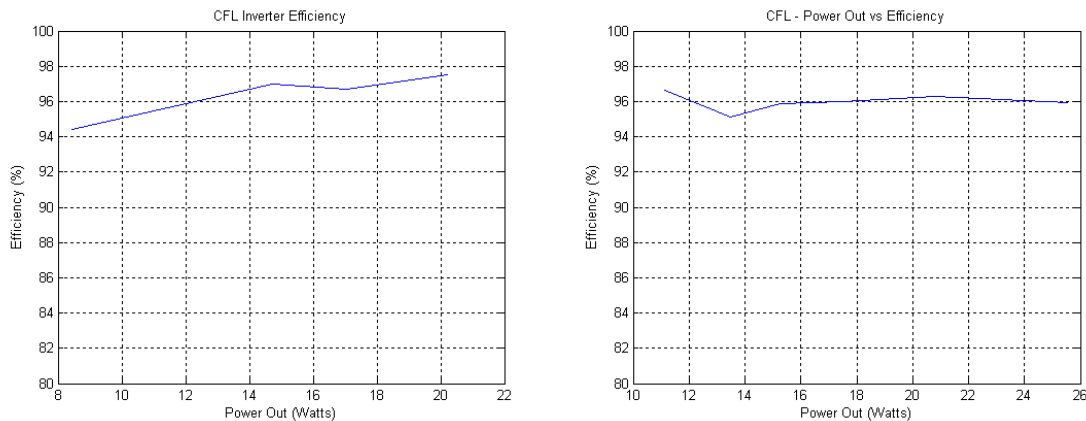


Fig.34 CFL Driver Efficiency

The CFL driver circuitry also proved to be efficient. The plots in Fig. 34 show a typical efficiency of 96% with a 25W load. The output signal also demonstrated a low harmonic content (Fig. 20). The CFL driver proved to be reliable when tested in the lab and was tested for several weeks prior to deployment to Remington Road with no failures.

However, the CFL driver did not perform as well as expected when deployed at Remington Road. Due to a miscommunication, the CFL driver was accidentally connected to the LED lamps, which caused major damage to the LED lamps and CFL driver. The LED lamps had to be replaced and major repairs were made to the CFL driver circuit. After the wiring mishap, the CFL driver had additional failures which were corrected later.

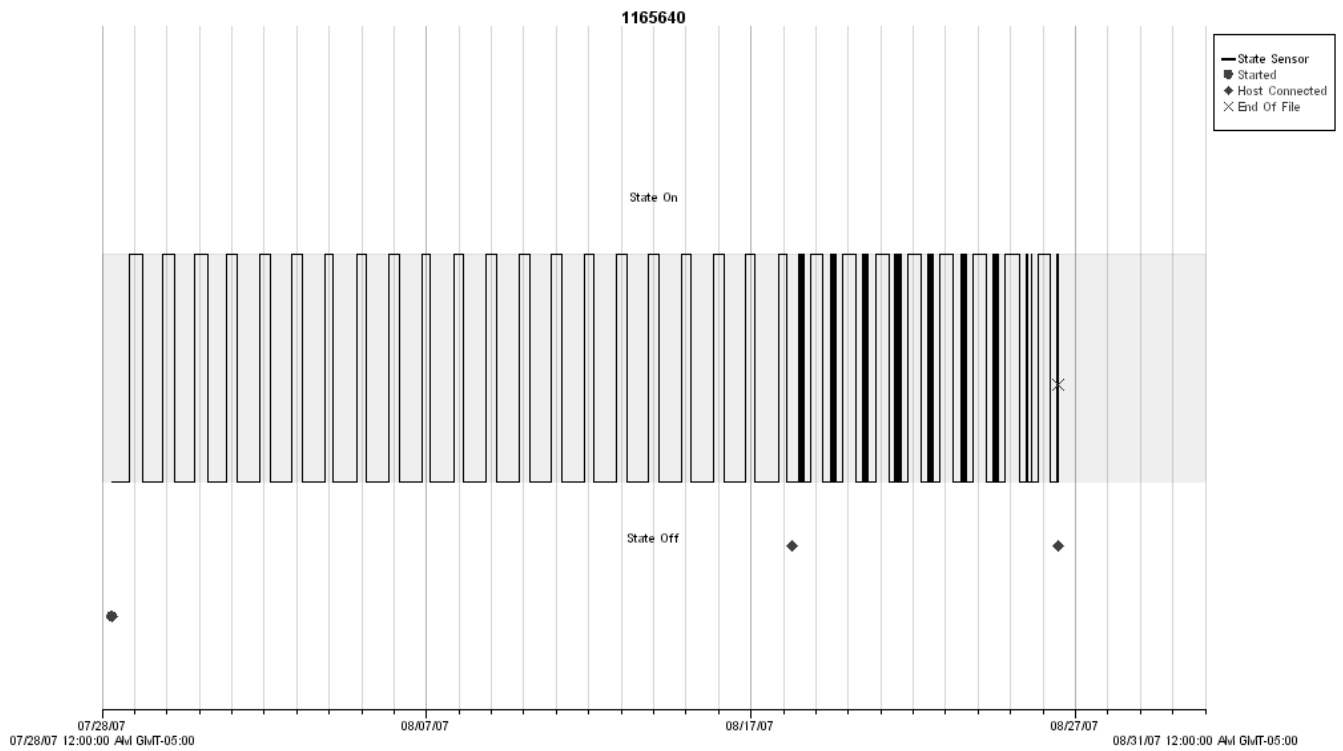


Fig. 35 CFL Data Logger – Data Set 1

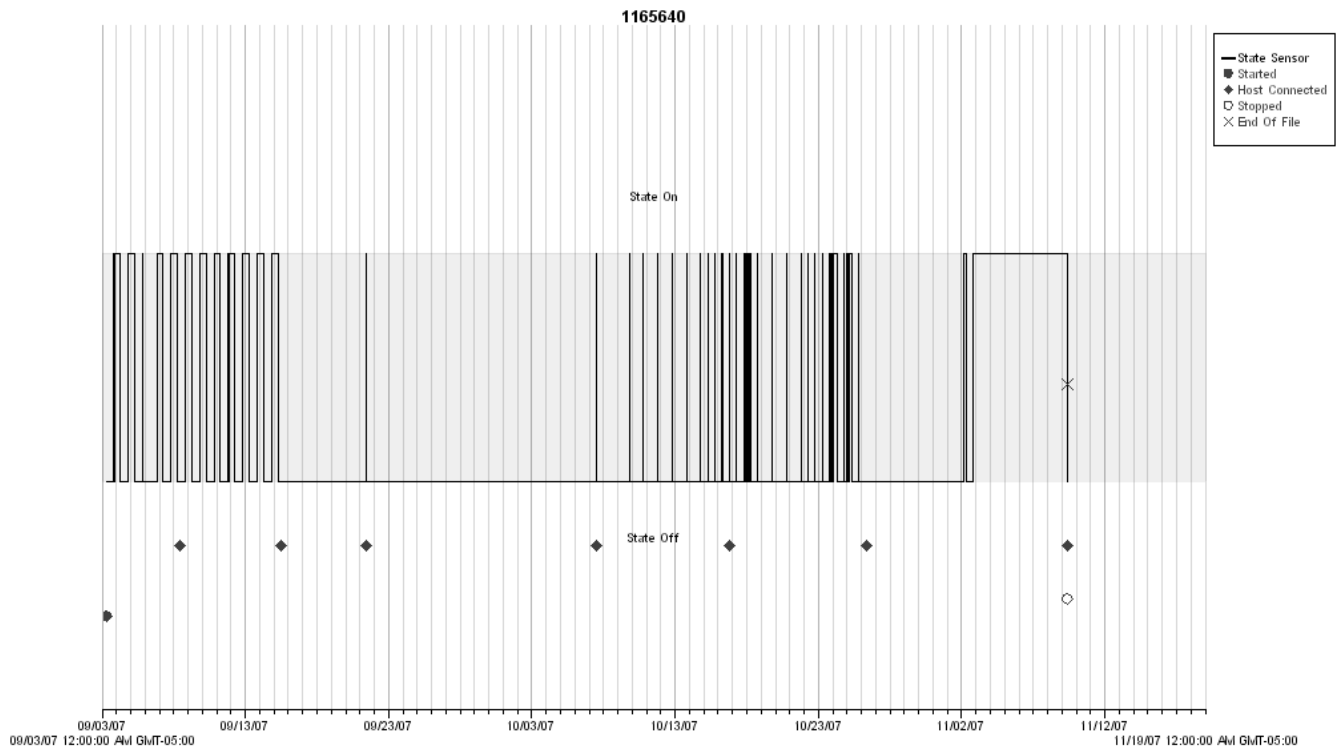


Fig. 36 CFL Data Logger – Data Set 2

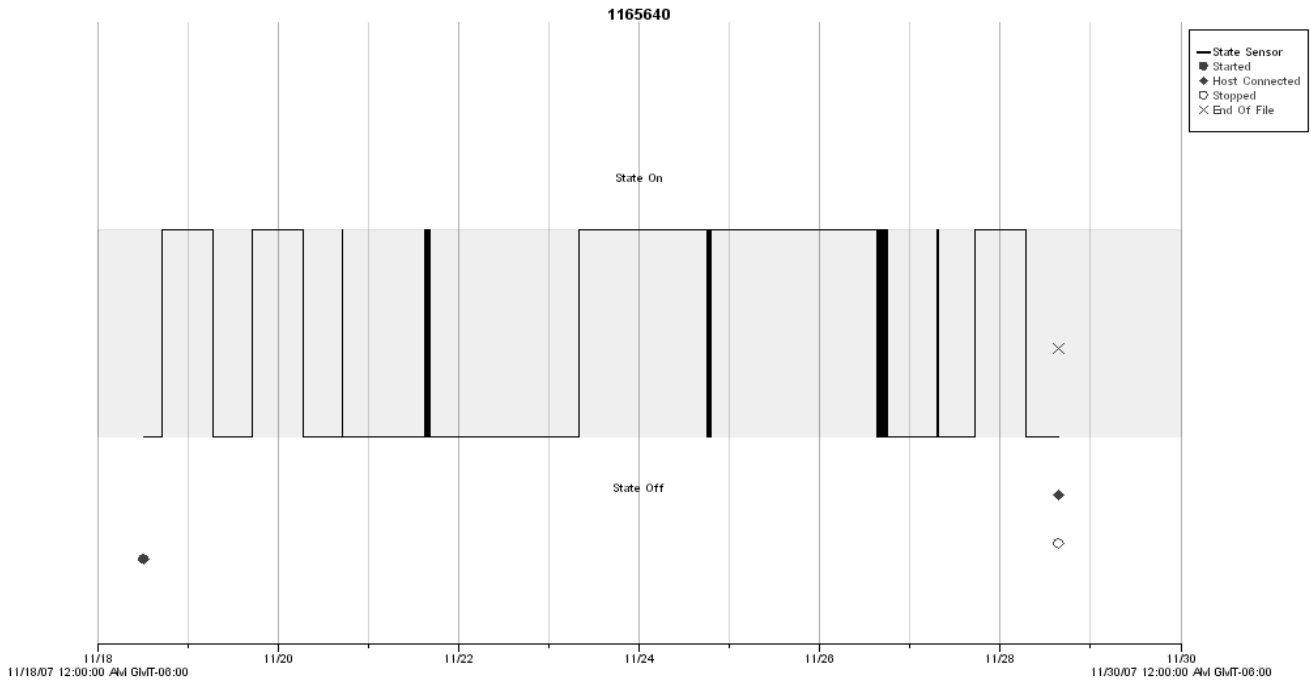


Fig. 37 CFL Data Logger – Data Set 3

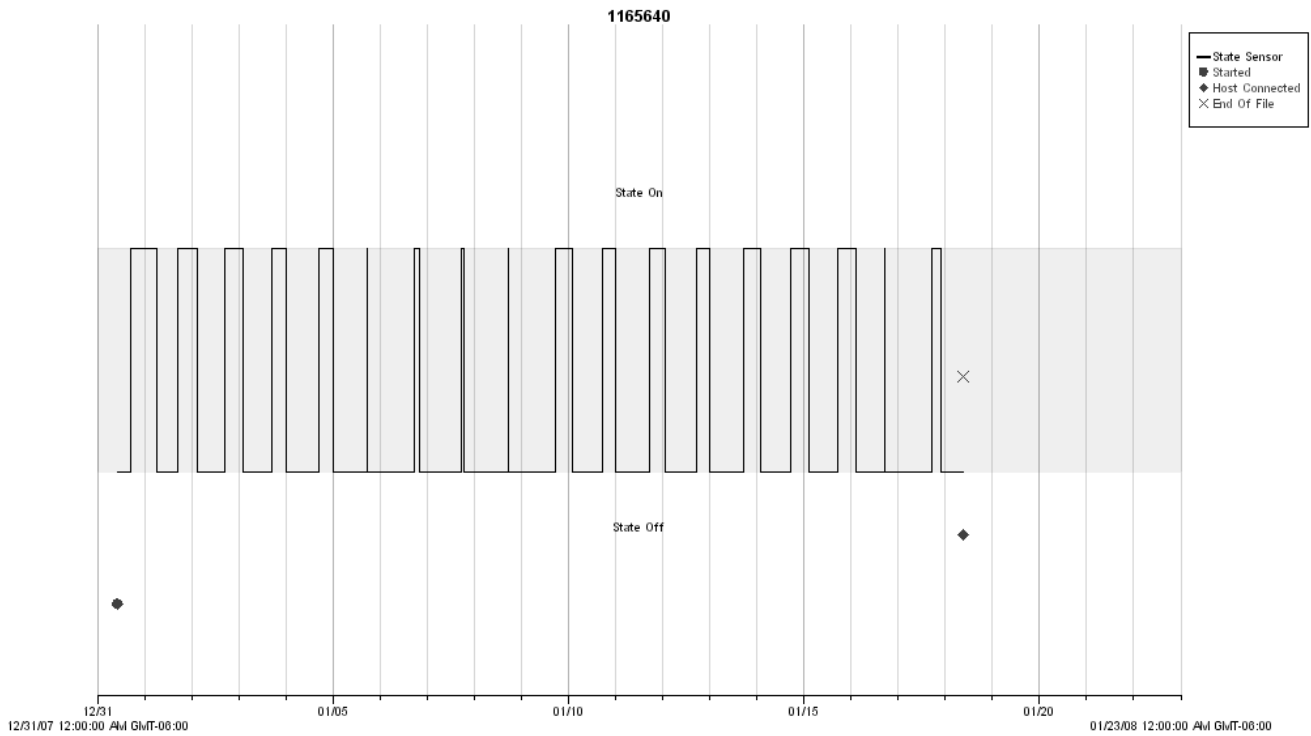


Fig. 38 CFL Data Logger – Data Set 4

The plots in Figures 35 – 37 show the on/off times of the CFL driver from July 27th through the end of November. Initially the CFL lights were on from about 8:30PM to 6:00AM (Fig. 35). A 45W solar panel was initially installed so that testing could begin, while waiting for the arrival of the 64W panel. The 45W solar panel being undersized for this application is reflected in the plot in Fig. 35. By August 17th, the lights were only staying on until 3:00AM.

Problems with the CFL driver began after a 64W solar panel with a new solar controller were installed on August 18th. The lights began to oscillate on and off during the day as the solar controller cut on and off as the batteries reached full charge (Fig. 35). In the original design, the solar panel voltage (via the solar controller) was used to detect when the lights should turn on and off. In the effort to bypass the solar controller, a wire was connected directly from the solar panel to the light detection circuit. Bypassing the solar controller also proved to be problematic (Fig. 36). Leakage through the solar controller from the battery bank to the solar panel caused a voltage to develop across the panel, which prevented the lights from turning on reliably. Component values were adjusted and a resistor was placed across the solar panel in the attempt to correct the problem. In the end, using the solar panel to detect when the lights should turn on proved to be unreliable because the solar panel output voltage varies under different loading conditions.

A separate phototransistor circuit was added to the lighting system for light detection, to avoid the problems associated with using the solar panel. The initial results were promising (Fig. 37), but there was a major failure in the battery bank circuitry around November 22nd. It is speculated that some of the components were wounded during the previous month as the system was continuously oscillating on and off.

VI. Further Explorative Research

The grant was given a six month extension until August 2008 at no supplemental cost. The extension was requested to give additional time to investigate *operation of CFL with dc source*. Such an approach for stand-alone solar application will be attractive since the dc to ac inverter can be eliminated reducing cost and also improve efficiency by eliminating inverter losses. However, the inverter design implemented earlier is universal in that it can drive any ac operated device. Two approaches were examined:

- Use of commercial type ballast with dc voltage.
- A modified ballast design for dc operation.

VI. 1 Commercial Ballast Operation with DC

A typical ballast circuitry employs a rectification circuit at the front end to convert ac supply voltage to a dc which is smoothed by a buffer capacitor. The dc voltage drives the electronic circuitry necessary to ignite the CFL. This is shown in Fig. 39.

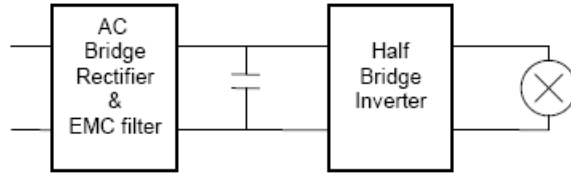


Fig. 39 Block Diagram of CFL Ballast

The input to the bridge rectifier is ac main. It also includes an EMC filter to reduce switching harmonics returning to ac main. One of the key components of the ballast is a high voltage IC designed to drive and control the CFL. It consists of a driver circuit for an external half bridge and bootstrap circuit; an oscillator; and timing & control circuit for start up, preheating, ignition, lamp burning and capacitive mode protection. The operating frequency of the circuit is approximately 40 kHz. Once the light bulb is ignited, the lamp's operating voltage and current drop and thus, make the CFL an energy efficient lamp.

With a view to eliminating the inverter that was employed previously, a new driver circuit was made ready and tested in the laboratory before installing at the field site on December 31st. The new driver circuit primarily consists of a series parallel conversion circuit for the batteries as shown in Fig. 15 with ancillary protection circuits. The data logger results are shown in the plot of Fig. 40 for the new system. It looks promising, although the CFL system is suffering from the same issue of the solar panel being shaded in the afternoon.

64 Watt Solar Panel

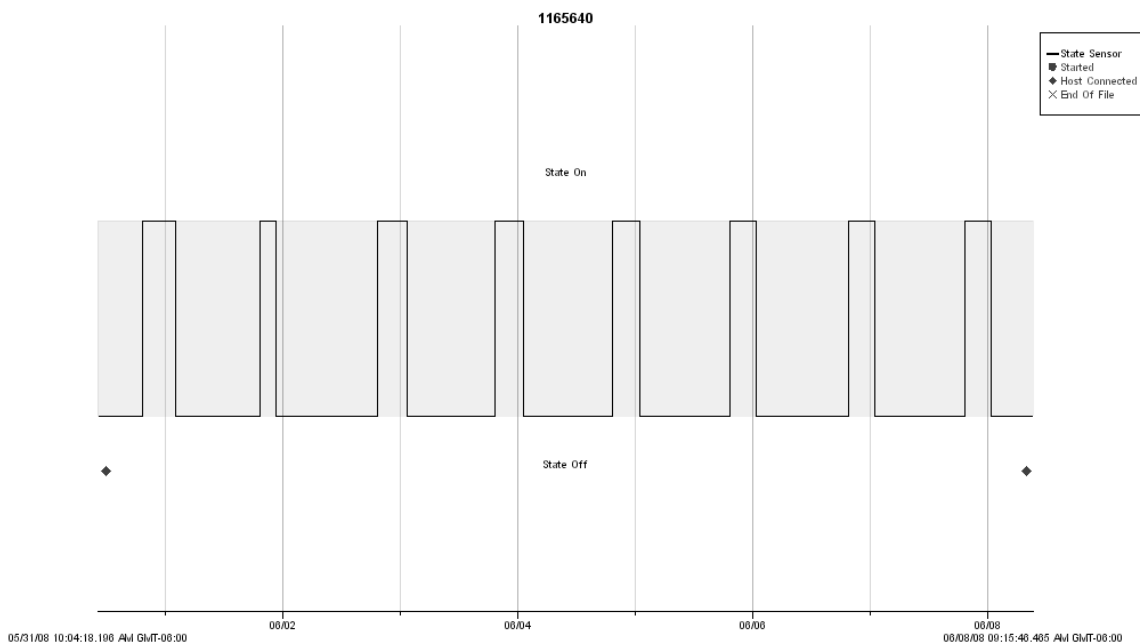


Fig. 40 CFL Data Logger Result: DC Driver

To mitigate the effect of afternoon shade on the solar panels, a 20W solar panel was added to the existing 64W panel for CFL. Highway department personnel installed couple of new posts and our student team designed the necessary frame to mount the new panel. A new start up company that visited the university informed us of their new product Apogee capacitor that may enhance solar charging of the batteries. The company gave us few sample units and was installed in parallel with the solar panel and the battery bank. These are very low ESR capacitors that have the characteristics of rapid charging. The initial results of adding the additional solar panel actually caused the ‘on’ time to decrease dramatically, which can be seen in Figure 41. It is believed that the solar controller experienced an over current condition causing an internal resettable fuse to open. Disconnecting the solar controller allowed the resettable fuse to close.

The maximum output of the solar panels is 5.2A, which is well below solar controller rated output of 7A. It is possible that the ambient temperature in the box that houses the solar controller may have allowed the resettable fuse to open at a current level below the solar controller’s rated output. The 7A rating is at 25 degrees Celsius. It is also believed that the Apogee capacitor that had been put in parallel with the batteries could have also contributed the high current condition. The capacitor has a very low ESR and may have allowed high current spikes to surge through the solar controller as the solar controller regulated its output voltage via PWM. Removing the capacitor and temporarily disconnecting the solar controller allowed the system to return to normal as seen in Figure 42.

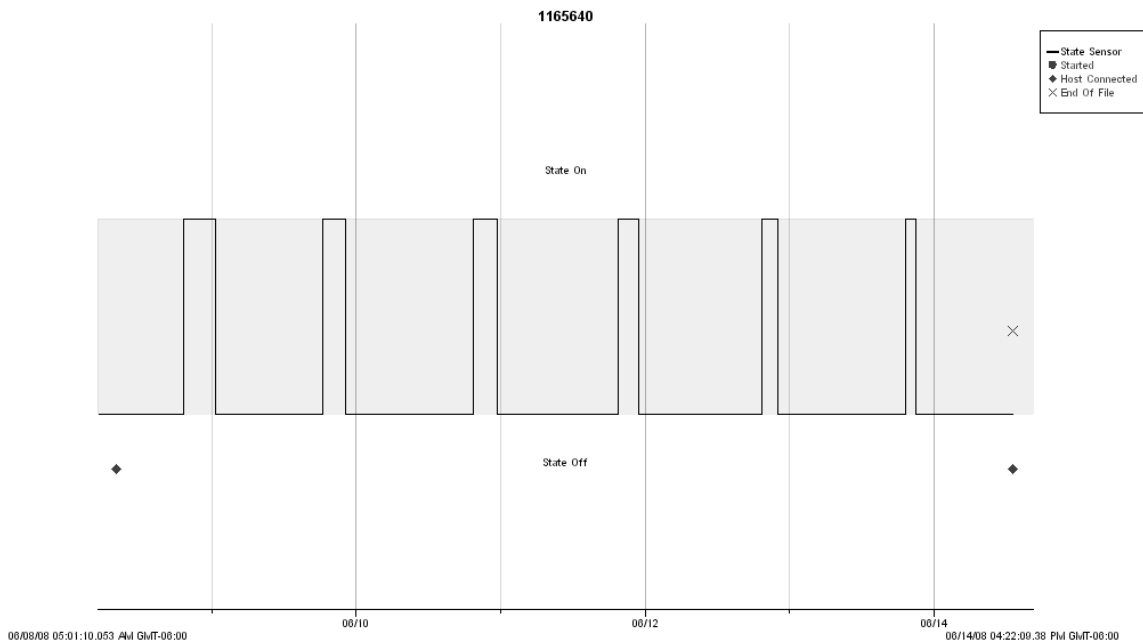


Fig. 41 CFL Light System: Adding 20 Watt Panel & Apogee Capacitor

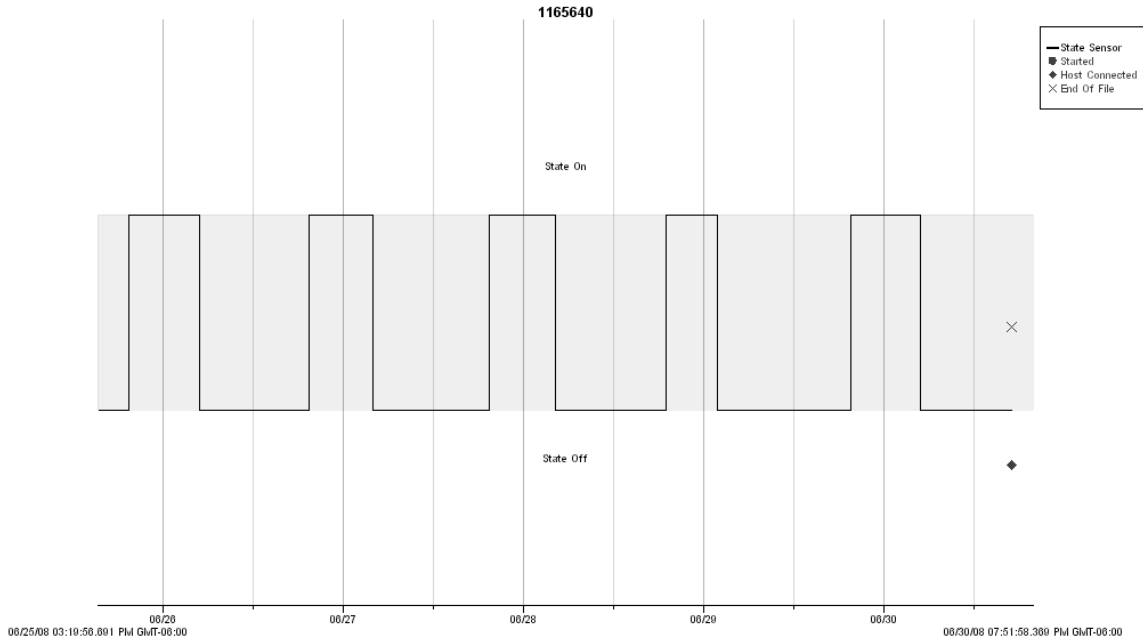


Fig. 42 CFL Light System: Removed capacitor and reset solar controller.

Towards the end of July and into August the CFL system ‘on’ time started to gradually decrease again. It is believed that the high ambient temperature in the summer months derated the 7A output rating of the solar controller allowing the resettable fuse to open at a lower current rating. It appears that the internal resettable fuse in the solar controller was opening prematurely as the temperature in the box, which houses solar controller, increased during the day preventing the batteries from reaching their fully charged state. As the sun rises, the output current of the solar panel increases and the temperature in the box increases until the resettable fuse opens. As the sun set, the solar panel output current level would drop below the hold current of the resettable fuse, allowing the fuse to close. This cycle repeated daily, preventing the batteries from receiving a full charge. On August 29th, the 7A solar controller was replaced with a more robust 10A solar controller. The last on/off data was collected on September 8th, approximately one week after installing the new solar controller. The plot shows that the ‘on’ time is increasing a small amount each day indicating the batteries are beginning to reach their full charge.

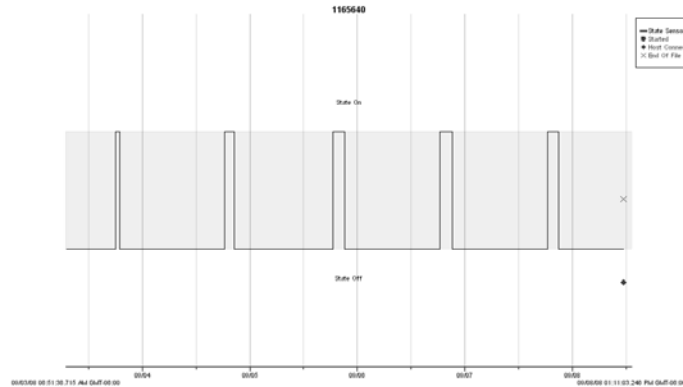


Figure 43 CFL Data Logger: 10A Solar Controller

VI. 2 A DC Driven Modified Ballast for 26W CFL

A third CFL lighting system was made ready and deployed for field testing at the home of the graduate student working on the project. The design modifies the reference design of the ballast IC IR2520D. The CFL driver circuitry is comprised of three major subsystems which include:

- Parallel/Series Battery Bank Connection

This is used to connect batteries in parallel during the day for charging & to connect the batteries in series at night to provide power to the CFL

- Voltage Doubler

A voltage doubler circuit was designed with a virtual ground to double the output voltage of the battery bank when in series operation to meet the high voltage requirement of IR2520D. In commercial application, this voltage is derived from the ac main.

- Electronic Ballast

The electronic ballast receives its voltage from the voltage doubler and converts to a high voltage 30 KHz – 50 KHz sine wave to drive the CFL

The voltage doubler and the electronic ballast schematics are shown in Fig. 44 and Fig. 45.

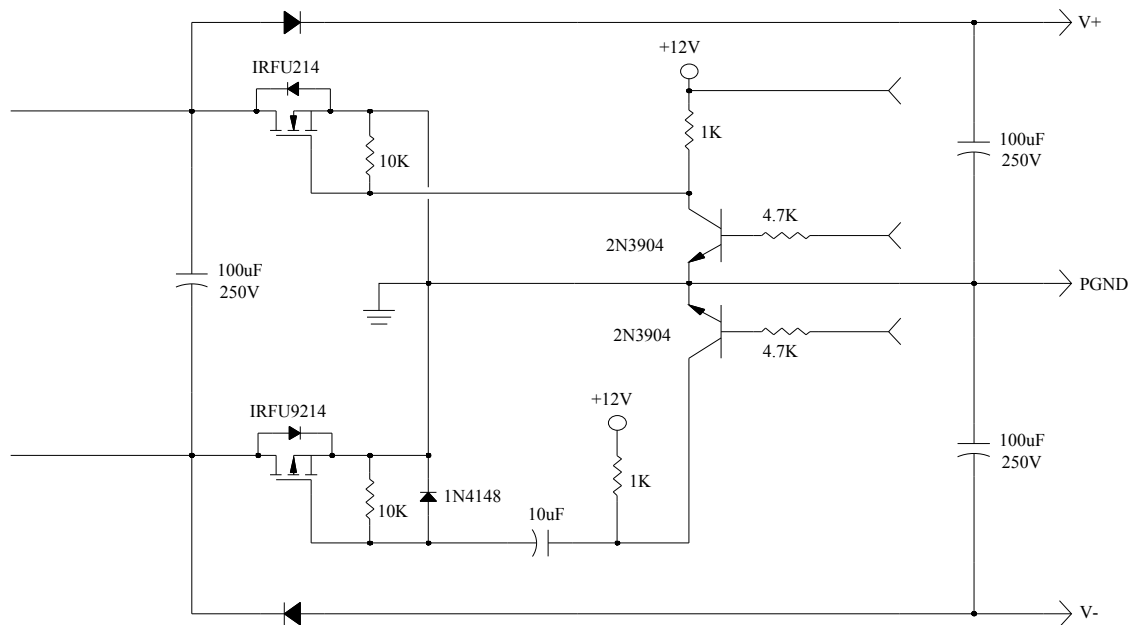


Fig. 44 Voltage Doubler

The input to the circuit of Fig. 44 is 144V dc (floating) from the battery bank. The inputs to the ballast in Fig. 45 are the three outputs from the doubler circuit.

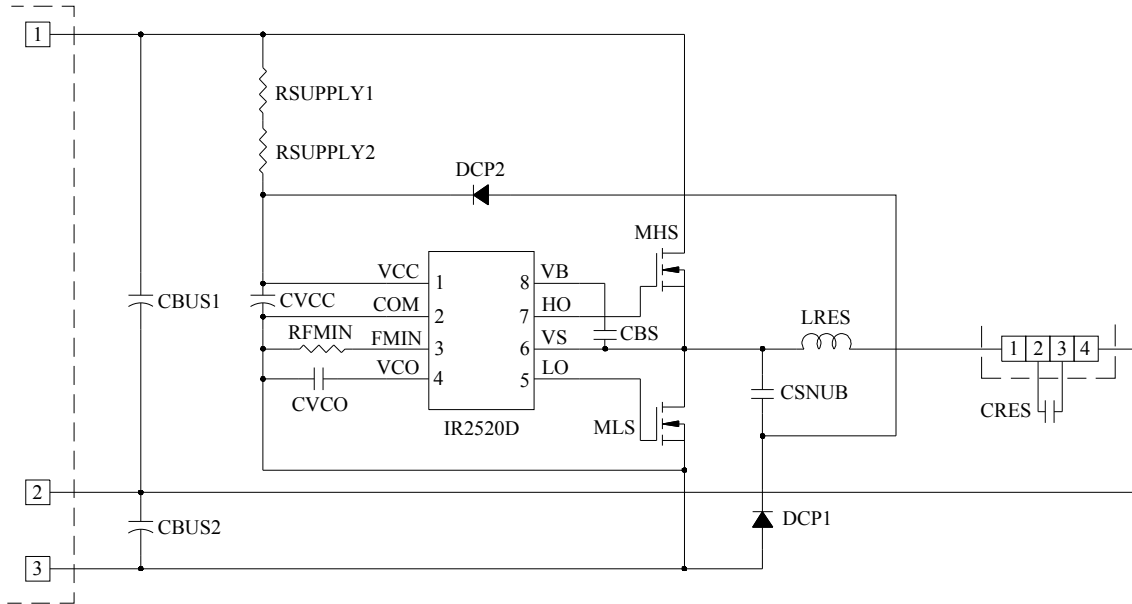


Fig. 45 Electronic Ballast

A printed circuit board (PCB) was designed to assemble all the components of the lighting system that employs a single 26W compact fluorescence lamp. This is shown in Fig. 46. The unit was housed in a plastic enclosure with a lid. The solar panel and the lighting effects are shown in Fig. 47 and Fig. 48. The lighting system was tested in the laboratory and showed promising results with a current draw of less than 200mA to illuminate the 26W CFL. In light intensity, a 26W CFL lamp is equivalent to $\approx 120W$ of incandescent lamp which would draw a current close to 1A.

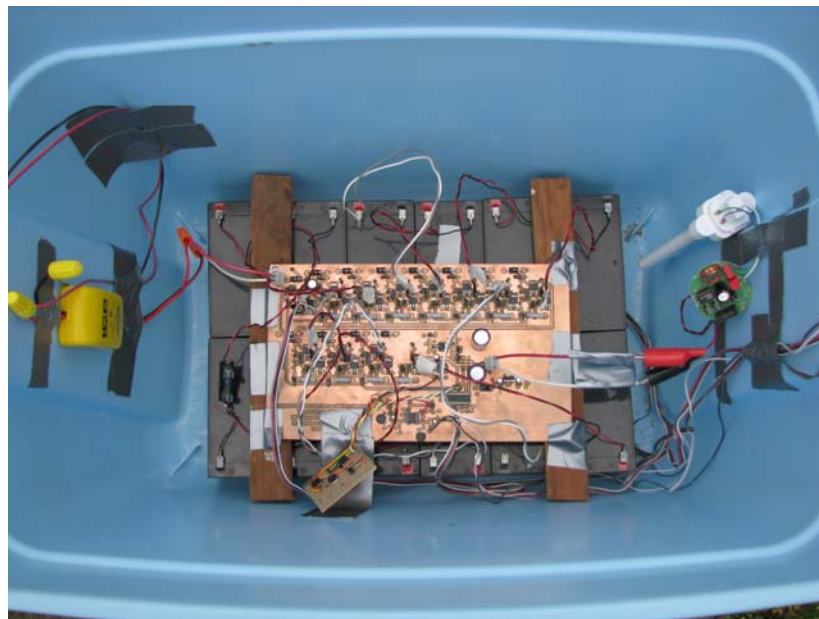


Fig. 46 26W CFL PCB & Light System Setup



Fig. 47 64W Solar Panel (Student's Backyard)



Fig. 48 26W CFL Setup at Night

An attempt was made to capture the on/off times with a data logger, but problems were encountered because of the virtual ground created by the voltage doubler. While a buffer circuit was being designed and fabricated, the CFL electronic ballast experienced an external storm failure that propagated component failures back through the parallel/series circuitry. The entire system showed excellent laboratory promise and warrants further investigation. The voltage doubler suffers the most losses ($\approx 80\%$ efficiency) and there are other approaches that should be investigated to improve efficiency. There was no time left within the scope of the grant to carry out further investigation. It is our belief that this aspect of the CFL design should be further explored and field-tested outdoor as second phase of the project. This will be an important contribution in the area of

harnessing solar energy efficiently for stand-alone applications. An eighteen month project will allow testing of the system in both summer and winter weather conditions.

VII. Project Conclusion

The primary goal of the project was to develop a low cost solution that harnesses solar energy to provide illumination of overhead highway signs. Two lighting systems were developed: one uses LED technology and the other is based on CFL technology. The CFL lighting for overhead sign has the advantage that light is uniformly distributed while LED emitted lights are directional. For stand-alone solar application, the implementation hardware is simpler for LED compared to CFL.

The LED light system design is based on a PWM (Pulse Width Modulation) strategy that drives two LED light fixtures. At the heart of this approach is a PIC microcontroller that controls the PWM switching of a pair of MOSFETs. The LED lights are time-division multiplexed at the rate of 1 KHz. The light fixtures were assembled with Lamina's LED light engines which consist of a dense cluster of multiple LEDs on a small substrate. This allowed for a high luminous intensity in a very small footprint. Weather proof commercial grade enclosures were used to mount the LED engines. Because of high power dissipation, heat sinks are necessary with LED drivers. The power storage unit consists of a 12V 20Ahr sealed lead acid battery which was charged by a 45W solar panel. A factor of 1:3 has been used in the sizing of the solar panel to account for short days and inclement weather conditions. Since the deployment of the unit with two fixtures on the 'Memphis Sign' (smaller sign) at Remington exit on I-40E, the lights have been working efficiently without any failure. The SLA battery needed replacement at one point due to a fault in charging circuitry and this has been corrected. Deep cycle battery, although expensive, will be our recommendation for the application.

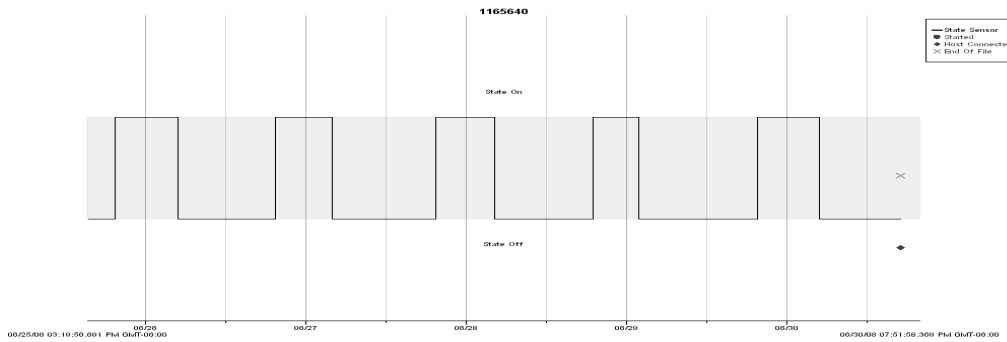
The first phase of CFL system design was focused on designing a highly efficient inverter for dc to ac conversion. The research on this has been highly successful with a new modulation strategy that has been published as 'Sectionalized PWM: A New Multilevel Modulation Strategy' in the literature [1]. The inverter efficiency is above 95% and its total harmonic distortion is less than 15%. A low distortion is essential if the inverter is connected to the grid. The inverter design employs twelve low amp-hr 12V SLA batteries with appropriate switching circuitry for their series-parallel connectivity. The batteries are connected in parallel during day for solar charging with a 64W solar panel, and they are placed in parallel for driving the inverter at night. The unit was deployed with three CFL lamps (8W each) which has the equivalent light emission of a 120W incandescent lamp. It was placed on the platform for the Remington Exit sign which has an area of 50 – 60 square feet. The few failures the system had were corrected and it worked efficiently turning on and off the lights at dusk and dawn. Slight changes in timing from day to day are caused by weather variation.

The second phase of CFL system design centered on its operation from 144V dc. The batteries when connected in series produced the high voltage. This voltage drove the CFL lamp directly without any inverter. The motivation for the approach is reducing cost and minimizing power loss. A PIC microcontroller was used to control the switches of a

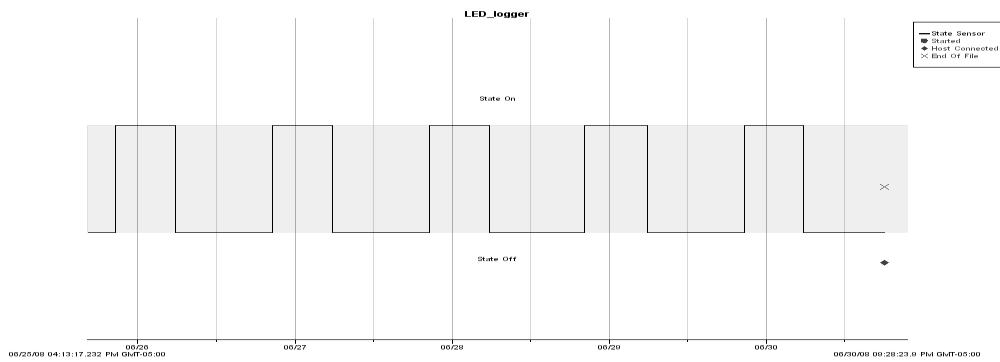
novel circuitry to connect the battery bank in series and parallel. The batteries are placed in parallel for solar charging. The unit had underperformed from time to time due to afternoon tree shading of solar panels and the effect of summer heat on the solar controller. An additional 20W panel was added and the solar controller capacity was increased. The system came back to normal after these changes, although it had some timing variations. The hysteresis in the control loop was adjusted to compensate for timing.

The third phase of CFL design was focused on implementation of ballast that would bypass ac to dc conversion and generate a high dc voltage internally through switching. The laboratory testing of the ballast with a 26W CFL gave very promising result with a high luminous efficacy. This is the best CFL efficacy we observed in the three methods that were investigated. There was no time left for field deployment of the unit. It is our recommendation that the unit be further developed with an improved voltage doubler circuit and the system field-tested to evaluate its outdoor performance. With the experiential knowledge we have, the extension of the work could be completed in a cost-effective manner with relative ease.

It can be concluded from our test results that the objectives of the project have been fully met, and even exceeded. The LED system is efficient for illuminating smaller sign board and the CFL system is better suited for large sign boards for its uniform light distribution. The latest improvements on ballast design would improve efficiency of the CFL driver circuitry. The following plots from data logger summarize the performance of the two systems.



CFL Performance Data



LED Performance Data

VIII. Research Publications Related to Project

- H. Patangia and D. Gregory, "A harmonic reduction scheme in SPWM," *Proc. IEEE APCCAS'06*, December 2006, Singapore
- H. Patangia and D. Gregory, "Implementation of a multilevel inverter for capacitive loads," *Proc. IEEE ICIT'06*, December 2006, Mumbai, India
- H. Patangia and D. Gregory, "A novel multilevel strategy in SPWM design," *Proc. IEEE ISIE'07*, June 2007, Vigo, Spain
- H. Patangia and D. Gregory, "High voltage signal processing using a small signal approach," *Proc. IEEE ISSPIT'07*, December 2007, Cairo, Egypt
- H. Patangia and D. Gregory, "Sectionalized PWM (S-PWM): A new multilevel modulation strategy," *Proc. IEEE ISCAS'08*, May 2008, Seattle, Washington

IX. References

- [1] H. Patangia and D. Gregory, "Sectionalized PWM (S-PWM): A new multilevel modulation strategy," *Proc. IEEE ISCAS'08*, May 2008, Seattle, Washington
- [2] D.G. Holmes and T.A. Lipo, *Pulse Width Modulation for Power Converters: Principles and Practice*. Hoboken, NJ: IEEE Press, 2003
- [3] J.R. Wells, P.I. Chapman, P.T. Krein and B.M. Nee, "Modulation-based harmonic elimination," *IEEE Trans. Power Electronics*, vol. 22, no. 1, Jan. 2007
- [4] J. Rodriguez, J. Lai, and F.Z. Peng, "Multilevel inverters: a survey of topologies, controls, and applications," *IEEE Trans. Ind. Electronics*, vol. 49, no. 4, Aug. 2002
- [5] M. Ma, L. Hu, A. Chen, and X. He, "Reconfiguration of carrier-based modulation strategy for fault tolerant multilevel inverters," *IEEE Trans. Power Electronics*, vol. 22, no. 5, Sep. 2007
- [6] H. Patangia, "Amplitude division multiplexing scheme in analog signal processing," *Proc. IEEE Int. Midwest Symp. Circuits & Systems*, Aug 2005, Cincinnati, Ohio